SYNTHESIS OF REDOX-RESPONSIVE HYDROGELS FOR CONTROLLED RELEASE OF THERAPEUTIC AGENTS

by

Ruveyda Kılıç

B.S., Chemistry, Boğaziçi University, 2016

Submitted to the Institute for Graduate Studies in
Science and Engineering in partial fulfillment of
the requirements for the degree of
Master of Science

Graduate Program in Chemistry
Boğaziçi University
2019

ACKNOWLEDGEMENTS

First of everything, I would like to thank my thesis supervisor Prof. Amitav Sanyal for taking me as a master student, giving me a chance to work on this comprehensive project, guiding and encouraging me throughout this journey.

I would also like to thank my thesis committee members, Prof. Rana Sanyal and Prof. Oğuz Okay for reading and reviewing my thesis. Especially, I am indebted to thank Prof. Oğuz Okay for helping me with the understanding of rubber elasticity theory and other concepts related to mesh size calculations.

Most importantly, I would like to express my gratitude to my family for their love, endless support, and patience.

I would also like to take this opportunity to thank my labmates and friends: Özgül Gök, Burcu Sümer Bolu, Merve Karaçivi, Aysun Değirmenci, Bianka Golba, and Nehir Kavak for being there for me all the time.

ABSTRACT

SYNTHESIS OF REDOX-RESPONSIVE HYDROGELS FOR CONTROLLED RELEASE OF THERAPEUTIC AGENTS

In recent years, hydrogels have attracted great attention for various biomedical applications ranging from chemical and biological sensing, delivery of therapeutic agents to tissue engineering. Reason for utilization of hydrogels for the aforementioned applications stems from our ability to design them with desirable physical and chemical characteristics. Properties like their high swelling in aqueous media, controlled biodegradation, biocompatibility, tailorable elasticity and porosity are among a few of such attributes. Tailoring the release characteristics of encapsulated therapeutic agents is crucial for many biomedical applications. To achieve a control over release profile, hydrogels with well-defined network connectivity are becoming popular due to their homogeneous inner structure. Crosslinking of well-defined multi-arm polymers with high efficiency provides a viable synthetic methodology to obtain hydrogels with better control over network structure. In this thesis work, we report the fabrication of well-defined hydrogels by reacting two different multi-arm polymers with complementary reactive groups in a fast and effective manner under environmentally benign conditions.

Hydrogels were fabricated by crosslinking of two different tetra-arm poly(ethylene glycol) based polymers, one containing pyridyl-disulfide and the other bearing thiol groups, in phosphate saline buffer, with gel conversions between 89-93%. Efficiency of the crosslinking process based on end group consumption analysis suggested chain coupling as high as 90-95%. Rheological and morphological characterizations revealed stable hydrogels with porous structures. It was demonstrated that the disulfide groups within the hydrogels undergo degradation in the presence of thiol-containing agents such as glutathione and DTT, to release the encapsulated therapeutic agents in a controlled or on-demand fashion.

ÖZET

TEDAVİ AJANLARININ KONTROLLÜ SALINIMI İÇİN REDOX-DUYARLI HİDROJELLERİN SENTEZİ

Son yıllarda, hidrojeller, kimyasal ve biyolojik sensörlerden, terapötik ajanların iletimi ve doku mühendisliğine kadar çeşitli biyomedikal uygulama alanlarında büyük ilgi toplamıştır. Hidrojellerin yukarıda belirtilen uygulamalardaki kullanım nedeni, hidrojelleri istenilen fiziksel ve kimyasal özelliklerde tasarlayabilme kabiliyetimizden kaynaklanmaktadır. Bu özelliklerden birkaçı; su içeren ortamlarda yüksek hacim artışı, kontrollü biyobozunma, biyouyumluluk, uyarlanabilir elastikiyet ve porlu yapı gibi özelliklerdir. Hidrojellerin içine hapsedilmiş terapötik ajanların salım profillerinin ayarlanabilir olması birçok biyomedikal uygulama için çok önemlidir. İyi tanımlanmış ağ bağlantılarına sahip hidrojeller homojen iç yapıları nedeniyle salım profili üzerinde bir kontrol elde etme bakımından popüler hale gelmektedir. İyi tanımlanmış çok kollu polimerlerin yüksek verimli çapraz bağlanması, ağ yapısının daha iyi kontrol edilebildiği hidrojellerin elde edilmesi için uygun bir sentez yöntemi sağlar. Bu tez çalışması ile, iki farklı çok kollu polimerin tamamlayıcı reaktif gruplarının çevresel açıdan zararsız koşullarda hızlı ve etkili bir şekilde reaksiyonu ile iyi tanımlanmış hidrojellerin üretilmesini bildiriyoruz.

Hidrojeller, biri piridil-bisülfit ve diğeri tiyol içeren iki farklı dört kollu poli (etilen glikol) kökenli polimerin çapraz bağlanmasıyla, fosfat salin tamponu içinde, % 89-93 arasında verim ile üretilmiştir. Çapraz baglama reaksiyonunun verimi, polimer uç grupların tüketiminin analizine dayanarak, zincir bağlantısının % 90-95 kadar yüksek bir oranda olduğunu göstermiştir. Yapılan reolojik ve morfolojik karakterizasyonlar, hidrojellerin porlu ve stabil bir yapıda olduğunu göstermiştir. Hidrojellerin, yapılarındaki disülfit gruplarının glutation ve DTT gibi tiyol-içeren ajanların varlığında bozularak, jel matrisine hapsolmuş terapötik ajanları kontrollü veya isteğe bağlı bir şekilde saldığı gösterilmiştir.

TABLE OF CONTENTS

LIST OF FIGURES

LIST OF TABLES

LIST OF ACRONYMS/ABBREVIATIONS

$CDCl_3$	Deuterated Chloroform
CH_2Cl_2	Dichloromethane
DMAP	4-Dimethylaminopyridine
DTT	Dithiothreitol
ECM	Extracellular Matrix
EDCI	1-Ethyl-3-(3-Dimethylaminopropyl) Carbodiimide
FDA	Food and Drug Administration
FITC	Fluorescein Isothiocyanate
GSH	Glutathione
HG	Hydrogel
kDa	Kilo Dalton
LVR	Linear-viscoelastic Limit Regime
Mc	Molecular Weight Between Crosslinking Points
MeOH	Methanol
NMR	Nuclear Magnetic Resonance
PBS	Phosphate Buffer Saline
PEG	Poly(ethylene glycol)
PLGA	Poly Lactic-co-glycolic Acid
pTSA	P-toluene sulfonoic acid
RGD	Arginylglycylaspartic Acid
rt	Room Temperature
SEM	Scanning Electron Microscopy
TEA	Triethylamine
THF	Tetrahydrofuran
UV	Ultraviolet
Vis	Visible

INTRODUCTION

1.1. Hydrogels

Hydrogels are defined as three dimensional polymeric networks which are cross-linked via physical and/or chemical interactions. Due to their porous structures, tunable viscoelastic behaviors and high water uptake capacities, hydrogels have attracted a growing interest in recent years. Hydrogel based materials play a significant role in a wide variety of research areas ranging from drug delivery systems, tissue engineering scaffolds to diagnostic platforms. Fabrication of hydrogels generally utilizes various predominantly hydrophilic building blocks such as monomers, polymers, cross-linkers, and solvents [1]. They can be designed with variability in their size e.g. from nanogels to macroscopic gels, as well as function e.g. stimuli-responsive swelling depending on the area of application.

Physically crosslinked hydrogels can be formed through association between polymer chains through hydrogen bonding, hydrophobic or ionic interactions [2]. Depending on external stimulating environments like temperature, ion concentration or pH of the medium, crosslinking or decrosslinking of polymers to switch between the gel and sol state can be achieved for these systems.

Chemically crosslinked hydrogels, on the other hand, are obtained through covalent crosslinking of polymer chains. As a widely used approach, polymers containing reactive functional groups e.g. hydroxyl, carboxylic acid, amine, alkene or alkyne groups are crosslinked using efficient coupling reactions such as Schiff-base formation, click chemistry based reactions, amidation, Diels-Alder cycloadditions and photo-induced crosslinking to yield chemically crosslinked hydrogels. Due to the stability of chemical bonds, covalently crosslinked hydrogels are preferred for applications where long term strength and durability is required. For example, polyethylene glycol/hyaluronic acid based hydrogels synthesized through the azide-alkyne cycloaddition click reaction can be obtained with mechanical and morphological compliance as filling materials is suitable for the bio applications such as plastic surgery [3].

Hydrogels can be formed using either natural and/or synthetic polymers. Hyaluronic acid, chitosan, heparin, alginate are the examples of most commonly used natural polymers, whereas polyethylene glycol (PEG), poly L-lactic acid, poly (lactic-co-glycolic acid), N-isopropylacrylamide are examples of frequently utilized synthetic polymer.

Hydrogels have attracted great attention recently due to their unique properties such as porosity, elasticity and absorption of large amount of water or biological fluids. These properties can be controlled by changing chemical composition of hydrogels. For example, hydrophilic polymers cause hydrogel to swell while hydrophobic components help controlling water uptake capacity and mechanical features.

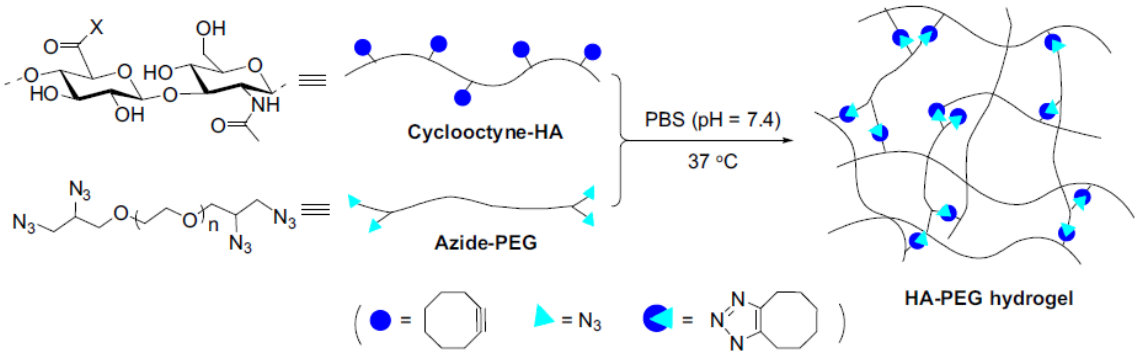

Figure 1.1. Hydrogel formation via Azide-Alkyne ‘’*Click Reaction*’’[4].

Stimuli sensitive hydrogels have emerged as desirable materials for various biomedical applications due to their controllable swelling/deswelling and degradation behavior. External stimuli such as pH, temperature, solvent and light can lead to changes in hydrogels’ structural or chemical properties, and thus provide handles to modulate properties of these materials [5], [6]. It is important to contemplate the necessity of hydrogels being non-immunogenic when biological applications are aimed. Hydrogel should not cause any inflammation in the implantation cite of the body. Therefore, natural polymers or synthetic polymers approved by regulatory authorities (*i.e*, FDA, EPA) are generally preferred. For example, PEG, PLGA, and PLA are synthetic polymers and collagen, alginate, and fibrin are natural polymers approved by FDA for clinical trials [7].

Biological applications of hydrogels range from their utilization as drug delivery systems, tissue engineering scaffolds, cell transplantation materials, wound healing bandages, diagnostic platforms, biomedication to biosensors [8].

For instance, PNIPAAm based polymers are among the most common ones used for obtaining temperature-responsive hydrogels [5]. For example, recently Wang *et al.* illustrated that a chemically crosslinked hydrogel containing of PNIPAAm allows controlled loading and release profile of a model drug because of its stimuli responsive nature [9].

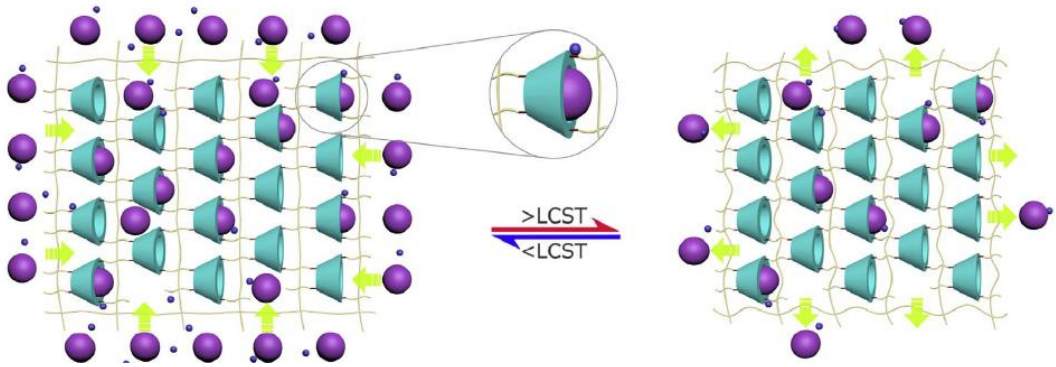

Figure 1.2. Temperature sensitive drug absorbance and release from NIPAAm containing hydrogels [9].

For the treatment of most diseases, it is important to have right dosage of therapeutic agents at the right place and at the right time. Keeping the effective drug concentration as required at the site of treatment is important in terms of side effects. Slow and controlled release of drugs can be achieved using stimuli-responsive hydrogels. The hydrogel matrix serves as a container for drugs and protects them from immune and digestive systems while allowing their passive diffusion over time or initiating a stimuli-induced diffusion.

Additionally, hydrogels, highly hydrated materials, provide a proper microenvironment to cells to live and proliferate by maintaining an attachment site for cell and allowing diffusion of small molecules like nutrition, oxygen, and metabolic byproducts [10]. They can act as wound dressings and improve healing of damaged tissue. They offer many advantages such as fluid absorption, hydration of the wound bed, cooling of the wound surface, quicker healing by helping reepithelization and reduced pain [11].

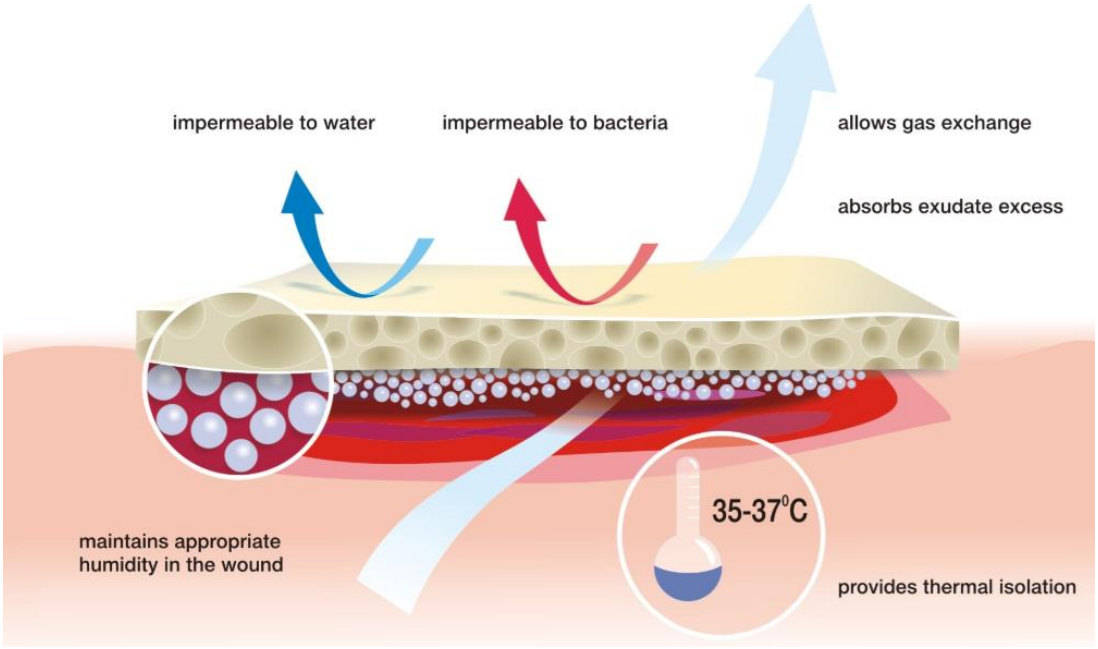

Figure 1.3 Schematic illustration of hydrogels as wound dressings [12].

1.2. Stimuli Responsive Cleavable Hydrogels

Hydrogels are among the widely employed materials in the field of drug delivery. Local delivery of drugs leads to dosage control and thus reduce systemic toxicity. Degradability of hydrogels plays an important role in regard to their biocompatibility, as well as controlled release of therapeutic agents. For this reason, environmentally sensitive hydrogels have great potential in numerous applications. These can be pH, temperature, light or enzyme sensitive cleavable hydrogels. Biomolecules such as glucose, oligopeptides (e.g. glutathione), and enzymes (e.g. matrix metalloproteinase) can also be employed as agents responsible of biodegradation [13], [14].

As an example of hydrogels responsible to biological cues, Anseth and coworkers reported a biodegradable hydrogel bearing human neutrophil elastase (HNE) sensitive linker. HNE is an enzyme that is abundant at inflammation sites in body, and thus can act as a cue for degradation to release therapeutic agent encapsulated within hydrogel. These hydrogels were fabricated using radical mediated thiol-ene photopolymerization reaction. Multi-arm norbornene end-functionalized PEG polymer were reacted with bis-cysteine

HNE sensitive peptides under UV-irradiation. Enzyme responsive controlled and tailorable release of model proteins bovine serum albumin (BSA) and carbonic anhydrase was realized in the presence of varying concentrations of HNE. Lastly, to indicate thiol-ene reaction does not show any deleterious effects on the activity of encapsulated molecules, lysozyme is used. Bioactivity of encapsulated lysozyme was calculated according to the activity of native lysozyme and retention of 93% of its activity is reported [15].

Additionally, biodegradable and biocompatible hydrogels can serve as cell scaffolds and carriers for tissue engineering because their physical and biochemical characteristics can mimic 3D structure of the natural extracellular matrix [16]. To generate a hydrogel suitable for cell encapsulation, mechanical properties and degradation profile must match with the natural extracellular matrix. Hydrogels derived from natural polymer precursors are subjected to rapid and facile degradation upon interaction with relevant body fluids via natural metabolic pathways. Synthetic polymers, on the other hand, cannot undergo degradation unless they carry enzyme specific domains or hydrolysable linkages such as amide and ester groups [17].

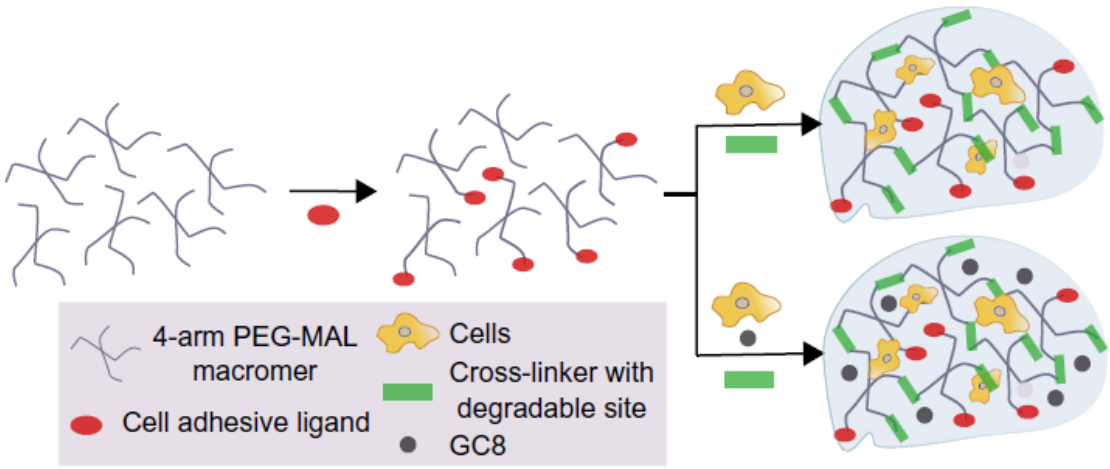

Figure 1.4. Cell encapsulation in hydrogels [18].

For example, Garcia and coworkers designed a biodegradable hydrogel by using multi-arm PEG macromers and a protease cleavable peptide containing dithiol cross-linker for cell encapsulation and delivery. First, they incorporated the cell adhesive ligand RGD to 4-arm PEG macromers in PBS. Then, RGD functionalized macromers were reacted with enzymatically cleavable peptide crosslinker. They used murine C2C12 myoblast cells for

encapsulation and showed that these hydrogels promoted increased spreading of encapsulated cells, using a live/dead assay [19].

Another way to form hydrogels with tunable swelling and rate-controlled degradation profile is through the combination of natural and synthetic polymers. For instance, Wang and coworkers synthesized a biodegradable hydrogel by crosslinking hyaluronic acid (natural) and PEG (synthetic) polymers through the thiol-disulfide exchange reaction. Enzymatic degradation is mediated by hyaluronidase (HAase), while reduction of disulfide linkages by glutathione provide a pathway for chemical degradation. A sustainable and high cell viability up to 7 days was observed for fibroblasts, endothelial and mesenchymal stem cells encapsulated within the hydrogel matrix [20].

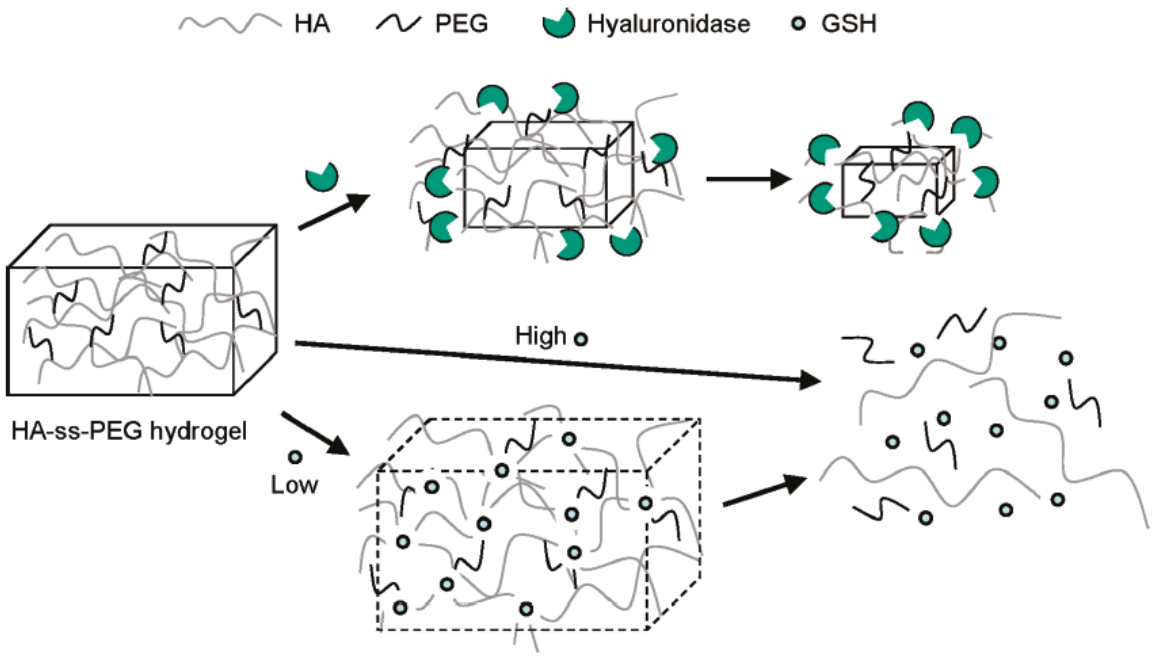

Figure 1.5. Schematic of biomolecule-triggered hydrogel degradation [20].

1.3. Well-Defined Hydrogels

Chemically crosslinked hydrogels can be classified as randomly crosslinked and well-defined network hydrogels depending on their chain connectivity. In randomly crosslinked hydrogels, polymer chains are inter-connected randomly and thus the chain

lengths between polymer junctions is not uniform. Due to the poor control over chain connectivity in random crosslinking, uneven distribution of crosslinking points and network defects (such as loose dangling chains) becomes unavoidable.

Randomly crosslinked hydrogels are mainly formed by photopolymerization. Photopolymerization is a traditional methodology to form 3D crosslinked materials. These reactions involving crosslinking telechelic polymers such as poly (ethyne glycol)-diacrylate oftentimes do not meet the chemical and physical requirements for biological applications. They demonstrate handicaps such as low stress tolerance, poor tensile strength, uneven and limited loading of drug molecule, besides, they can undergo bulk erosion and cause unexpected burst release [21], [22].

In 2006, Hawker, Hedrick and coworkers introduced novel hydrogels synthesized by 'click' chemistry, where they demonstrated a well-defined network structure with controlled architecture and improved mechanical properties. They functionalized linear PEG polymers with diacetylene and used a tetra-azide based crosslinker to obtain hydrogels through Cu(I) -catalyzed alkyne-azide cycloaddition reaction. A high gelation yield and improved tensile strength is achieved due to the near ideal network structure [23].

In 2009, Yang and coworkers synthesized a PEG based hydrogel for cell-based wound healing applications. In brief, triple bond bearing 4-arm PEG polymers were reacted with a RGD containing peptide bis-azide in an equimolar functional group stoichiometry in an aqueous media, in the presence of Cu-catalyst to yield well-defined hydrogels. They reported a fast and efficient gelation. Addition of RGD containing peptide sequence as a crosslinker enabled improved human dermal fibroblast cell attachment onto the hydrogels thus indicating potential for application of these materials as cell carriers for tissue regeneration purposes [24].

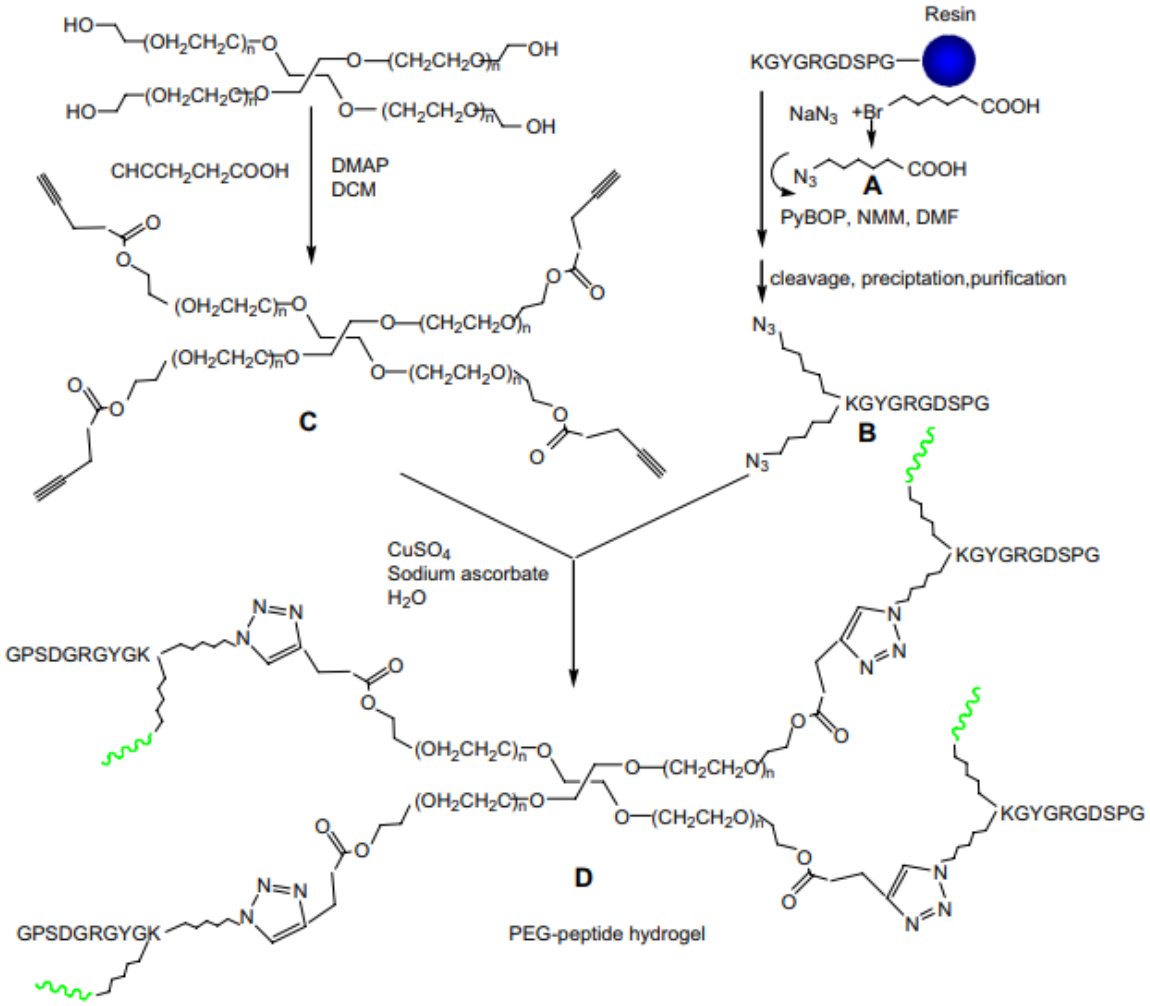

Figure 1.6. Synthesis of well-defined PEG-peptide hydrogel via click chemistry [24].

In another example of near-ideal network hydrogels, Sanyal and coworkers synthesized a oligo(ethylene glycol)-based cyclodextrin containing hydrogel for loading and controlled release of puerarin, a hydrophobic drug used in glaucoma. They obtained hydrogels via the radical mediated thiol-ene reaction with a good thiol-consumption percent, suggesting good control over network structure. A sustained release of the poorly water-soluble drug was observed and association of the drug with the hydrophobic cavity of cyclodextrins was attributed as a possible reasoning. Moreover, the thermo-responsive behavior of polymers with pendant oligo(ethylene glycol) chains was used to decrease the burst release through collapse of network at near physiological temperature [25].

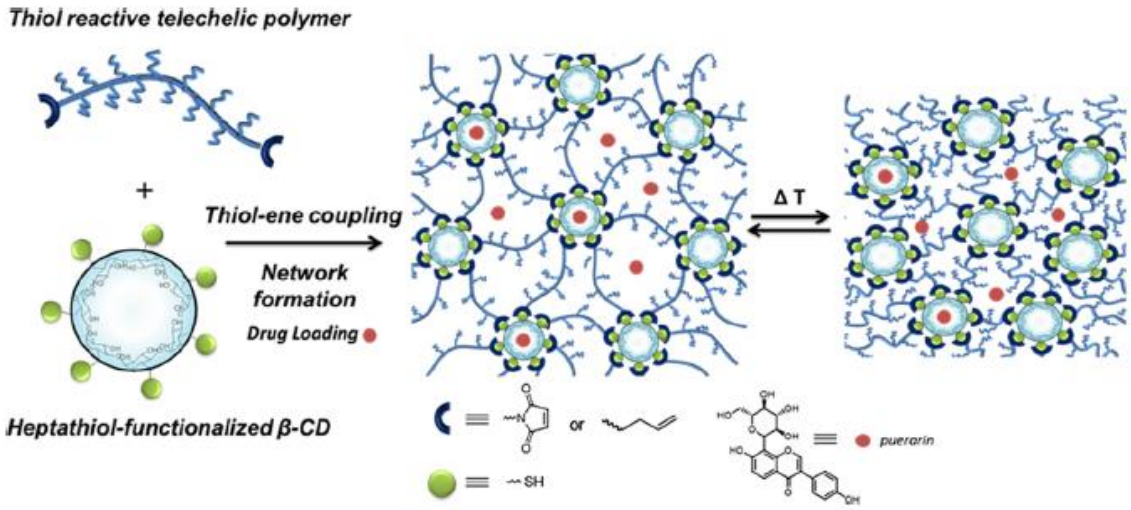

Figure 1.7. Illustration of thermoresponsive hydrogel fabrication via Thiol−Ene addition reaction and its drug-loaded state [25].

1.4. Hydrogels via Thiol-Disulfide Exchange Reaction

Biomaterials bearing disulfide functional group have drawn growing attention in biological applications due to their redox-responsive behavior. They are prone to degradation in the presence of reducing agents such as thiol-containing peptides e.g. glutathione which is abundant in the human body. Disulfide group displays no cytotoxicity against heathy tissue since it is commonly found in biological systems, for example, tertiary structures of various proteins are stabilized via disulfide bridges. Since the disulfide bonds under cleavage in a very selective manner i.e. predominantly when exposed to elevated levels of thiols, biomaterials containing disulfide linkers are investigated for many applications such as drug delivery and tissue engineering [26], [27].

In 2015, Varghese and coworkers synthesized hydrogels using bis-acrylate PEG-based polymers containing disulfide moieties on their backbone. Hydrogel formation is achieved via UV-mediated photo-polymerization and disintegration is expected to happen from cleavage of the disulfide bonds when exposed to cell-secreted thiol-containing peptides such as glutathione. Human mesenchymal stem cells (hMSCs) and human induced pluripotent stem cells (hiPSCs) were encapsulated within the PEG-diacrylate hydrogel and cultured in corresponding growth medium. Successful encapsulation of stem

cells into stable hydrogel scaffold and high cell viability was demonstrated. An autonomously controlled degradation of these hydrogels by the embedded cells and controlled release of the encapsulated cells to the host tissue was successfully accomplished [14].

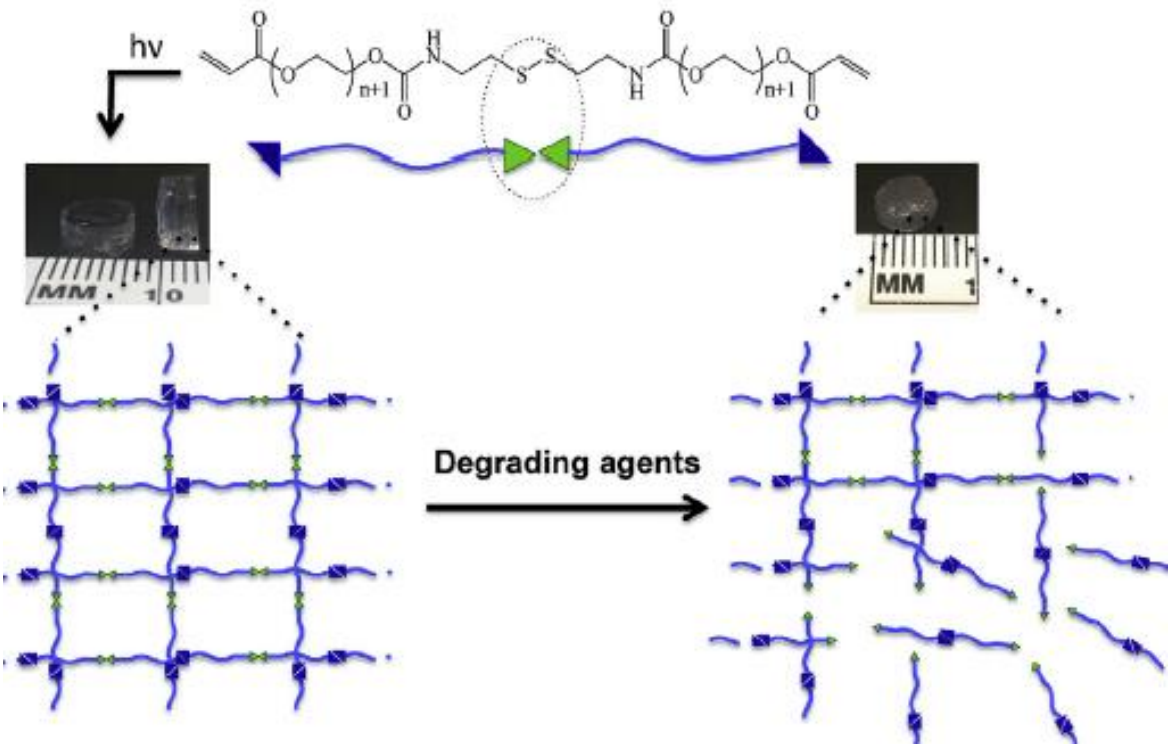

Figure 1.8. Degradation of hydrogel via disulfide reduction [14].

Another example of stimuli sensitive degradable disulfide bearing hydrogels was reported by Sinko and coworkers in 2011. In this work, disulfides are located on crosslink junction points; thus, it is aimed to crosslink and degrade hydrogel at these points. They used two different approaches to obtain disulfide linkages; first method is the oxidation of octa-thiol functionalized 8-arm PEG polymers in the presence of an oxidizing agent, H_2O_2, second, they have employed thiol-disulfide exchange reaction. Properties like gelation rate, drug encapsulation efficiency, and degree of swelling compared for two kinds of hydrogels. Shortly, the gel synthesized via thiol-disulfide shuffling showed slightly better properties like improved drug loading which can be explained by the nature of pore formation. Thiol-oxidation gel displays a collapsed structure while disulfide exchange reaction requires a stretching of polymer branches to crosslink with other polymer chains. They used doxycycline, an antibiotic used for bacterial infections, as a model drug and its

sustained release up to 10 days is reported. As a summation, poly (ethylene glycol) based reversible crosslink disulfide linkage bearing hydrogels are reported as dermal wound healing biomaterials in this work [28].

In 2017, Zhang and coworkers used disulfide chemistry to synthesize injectable self-healing hydrogels. They reacted thiol functionalized thermo-responsive triblock copolymer F127 and dithiolane modified PEG together at physiologic temperature. In addition to thermo sensitivity of F127 polymer, pH dependence of thiol-disulfide exchange reaction is also employed to modulate physical properties of hydrogels. Due to the reactivity of the disulfide bonds in hydrogel, a self-healing property is achieved and proved by rheological analysis such as repeated dynamic strain step tests [29].

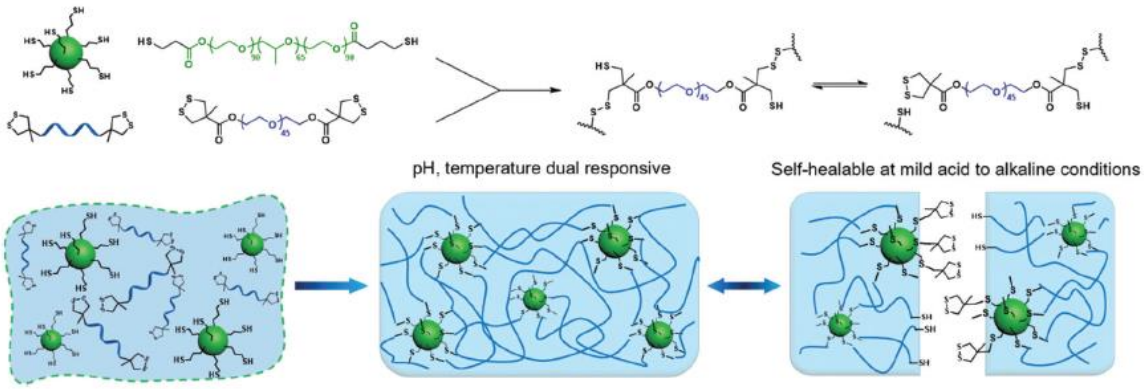

Figure 1.9. Schematic illustration of the injectable self-healing hydrogel fabricated via thiol/disulfide exchange reaction [29].

2. AIM OF THE STUDY

In this research, a novel biodegradable and biocompatible carrier platform is designed for biomedical applications such as drug delivery and tissue engineering. Well-defined PEG-based hydrogels are synthesized and characterized for this purpose. Biodegradability is ensured through installation of stimuli responsive cleavable disulfide linkages within the hydrogel matrix. Poly(ethylene glycol) (PEG) based polymers were chosen for their non-immunogenic, biocompatible and hydrophilic nature. Thiol-disulfide exchange reaction was used as a preferred method for crosslinking of the polymers since it does not require any metal based catalyst or special reaction conditions such as UV-irradiation.

Pyridine disulfide functionalized tetra-arm PEG polymer is reacted with PEG-tetra thiol polymer in PBS (pH 7.4) at physiological temperature. Not only is the chemistry utilized environmentally safe, but also proceeds with fast kinetics in a highly specific manner to yield gelation in a one pot reaction. Starting from the synthesis of appropriately functionalized tetra-arm polymers, hydrogels are obtained. End group conversion, swelling, degradation, rheological analysis, and lastly encapsulation and controlled release of FITC-Dextran, a model macromolecule, is undertaken in this thesis work.

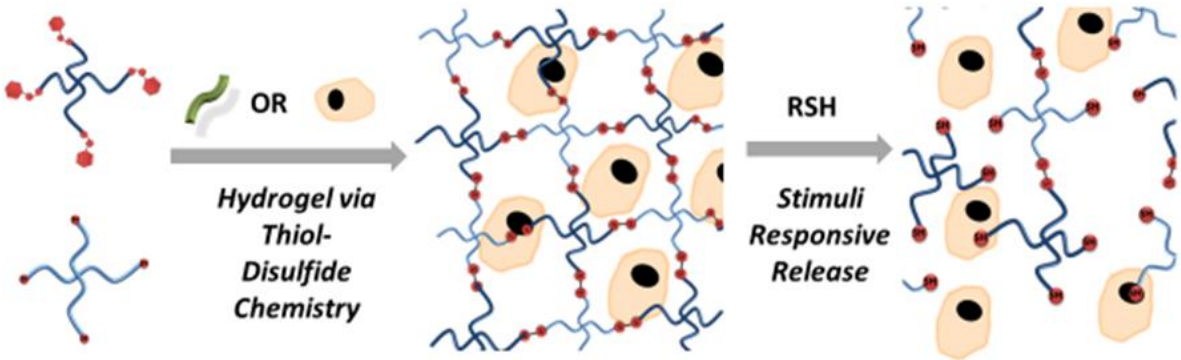

Figure 2.1. General illustration of the hydrogel synthesis, entrapment of desired cargo and release upon stimuli sensitive degradation.

3. EXPERIMENTAL

3.1. Materials and Methods

Poly (ethylene glycol) with molecular weights of Mn = 10000 and 20000 g/mol, were purchased from Creative PEG Works. *N*,*N*-Dimethylpyridin-4-amine (DMAP), mercaptopropionic acid, glutathione (reduced), 5,5′-dithiobis(2-nitrobenzoic acid) (Ellman's Reagent), p-toluenesulfonoic acid monohydrate (pTSA), 2-aldrithiol, 2-mercaptoethanol, glacial acetic acid, succinic anhydride, FITC-dextran (Mn= 20 and 150 kDa), and triethylamine (TEA) were purchased from Sigma-Aldrich and used as received. 1,4-Dithiothreitol (DTT) and *N*-ethyl-*N*′-(3-dimethylaminopropyl) carbodiimide hydrochloride (EDCI) were purchased from Alfa Aesar. 2-(2-Pyridinyldithio) ethanol and 4-arm poly (ethylene glycol) tetra-thiol (PEG-4SH) were prepared according to literature procedure [30], [31]. Solvents were obtained from Merck Co. (Germany) and used as received. Anhydrous tetrahydrofuran (THF), toluene, and dichloromethane (DCM) were obtained from SciMatCo purification system.

3.2. Measurements and Characterization

^{1}HNMR spectroscopy (Bruker 400 MHz) was used to characterize functionalized polymers. Fluorescein isothiocyanate (FITC) labeled dextan release from hydrogels was analyzed using a Varian Cary 100 Scan UV/vis spectrophotometer. Removal of water from hydrogels was accomplished with LabConco lyophilizer. Morphologies of dried gels were investigated with JEOL NeoScope JCM-5000 scanning electron microscopy (SEM) instrument at an accelerating voltage of 10 kV. The rheological behaviors of hydrogel samples were characterized in terms of loss (G″) and storage (G′) moduli of hydrogel samples equilibrated in water by measuring the angular frequency dependence of modulus values using an Anton Paar MCR 302 rheometer. To avoid solvent evaporation during measurements, a solvent trap was used.

3.3. Synthesis of 4 arm 10k-PEG-COOH (P1)

Tetra-arm PEG (M_n=10000 g/mol) was dissolved in toluene and dried by azeotropic rotary evaporation and then left under vacuum overnight before use. Dried PEG (0.5 g, 0.05 mmol) and TEA (0.04 mL, 0.29 mmol) were mixed in anhydrous THF (0.2 mL) under a N_2 atmosphere. Succinic anhydride (0.11 g, 1.0 mmol) and DMAP (0.0048 mg, 0.04 mmol) were completely dissolved in anhydrous THF (1.8 mL) at room temperature under N_2 atmosphere. The succinic anhydride containing solution was transferred slowly into the PEG solution using a syringe. The solution was stirred at room temperature under N_2 atmosphere for 20 h. Thereafter, the reaction solution was concentrated by removing solvent under reduced pressure. The PEG diacid was precipitated in cold diethyl ether. The precipitates were dissolved in dichloromethane and then reprecipitated two times in cold diethyl ether. The precipitates were collected and dried under vacuum. The product (**P1**) was obtained as a white powder with 70% yield and over 90% end group conversion according to ^{1}H NMR spectroscopy (Figure 4.2). ^{1}H NMR ($CDCl_3$, δ, ppm) 2.64 (m, 16H, OCC*H*$_2$C*H*$_2$COOH), 3.4-3.8 (m, 909H, OC*H*$_2$C*H*$_2$), 4.25 (m, 8H, C*H*$_2$OCO).

3.4. Synthesis of 4 arm 20k-PEG-COOH (P2)

Using the procedure outlined above, the tetra-arm PEG Mn=20000 g/mol based tetra-acid derivative was synthesized. The product (**P2**) was obtained as a white powder with 80% yield and near quantitative end group conversion according to ^{1}H-NMR spectroscopy (Figure 4.3). ^{1}H NMR ($CDCl_3$, δ, ppm) 2.64 (m, 16H, OCC*H*$_2$C*H*$_2$OC), 3.4-3.8 (m, 1818H, OC*H*$_2$C*H*$_2$), 4.25 (m, 8H, C*H*$_2$OCO).

3.5. Synthesis of 2-(2-Pyridinyldithio)ethanol (PDS-OH)

2-(2-Pyridinyldithio)ethanol was synthesized according to a previously reported literature procedure. [30] Briefly, aldrithiol-2 (2 g, 9.0 mmol) was dissolved in 6 mL of methanol with glacial acetic acid (0.12 mL, 2.27 mmol). In another flask, 2-

mercaptoethanol (0.31 mL, 4.5 mmol) in methanol (2 mL) were mixed and added onto the aldrithiol-2 solution drop by drop by a syringe at room temperature and the reaction was stirred for 3 h. Thereafter, methanol was evaporated under reduced pressure. The yellow oily crude product was purified by extraction (DCM: H_2O, 1:1 v/v), then, column chromatography was used to obtain pure 2-(2-pyridinyldithio) ethanol (ethyl acetate/hexane as eluent and silica gel as a stationary phase). The polarity of the eluent was increased until excess aldrithiol-2 came out and then it was kept constant until all aldrithiol-2 was collected, followed by rinsing the column with ethyl acetate to collect the desired product in its pure product with an overall yield of 70%.

3.6. Synthesis of 4 arm 10k-PEG-PDS (P3)

Previously synthesized and azeotropically dried polymer **P1** (0.4 mg, 0.04 mmol) was dissolved in anhydrous DCM (1 mL). Pyridyl disulfide alcohol (PDS-OH) (0.14 mg, 0.7 mmol), EDCl (0.032 mg, 0.16 mmol), and DMAP (0.0018 mg, 0.015 mmol) were dissolved in anhydrous DCM (2 mL) at room temperature and the mixture was added in a dropwise manner into the solution containing the P1 polymer under N_2 atmosphere. The reaction mixture was left for 20 h at room temperature with stirring under N_2 atmosphere. At the end of the reaction time, solvent was removed under reduced pressure. Residue was extracted with DCM (30 mL) and saturated $NaHCO_3$ (60 mL) three times. All DCM fractions were collected and removed under reduced pressure, and residue was precipitated in cold diethyl ether. The precipitates were collected and dried under vacuum. The product (**P3**) was obtained as a white powder with 80% yield and 95% end group conversion according to ^{1}H NMR analysis (Figure 4.6). ^{1}H NMR ($CDCl_3$, δ, ppm) 2.64 (m, 16H, OCC*H*$_2$C*H*$_2$OC), 3.03 (t , J=12.78, 8H, SC*H*$_2$), 3.4-3.8 (m, 909H, OC*H*$_2$C*H*$_2$), 4.25 (t, J= 9.05, 8H, C*H*$_2$OCO), 4.34 (t, J=21.8, 8H, C*H*$_2$OCO), 7.11 (d, J=11.8, 4H, NCC*H*), 7.58-7.68 (m, 8H, CHC*H*C*H*N), 8.45 (d, J= 4.23 Hz, 4H, C*H*N).

3.7. Synthesis of 4 arm 20k-PEG-PDS (P4)

Azeotropically dried **P2** (0.2 mg, 0.02 mmol) was dissolved in anhydrous DCM (1 mL). Pyridyl disulfide alcohol (PDS-OH) (0.036 mg, 1.9 mmol), EDCl (0.0082 mg), and DMAP (0.0009) were dissolved in anhydrous DCM (2 mL) at room temperature and added dropwise into the solution containing polymer **P2** under N_2 atmosphere. Reaction mixture was stirred at room temperature for 20 h under N_2 atmosphere. At the end of the reaction, solvent was under reduced pressure. The obtained residue was extracted with DCM (30 mL) and saturated $NaHCO_3$ (60 mL) three times. All DCM fractions were collected and removed under reduced pressure, and residue was precipitated in cold diethyl ether. The precipitates were collected and dried under vacuum. The product (**P4**) was obtained as a white powder with 80% yield and 82% end group conversion according ^{1}H NMR analysis (Figure 4.7). ^{1}H NMR ($CDCl_3$, δ, ppm) 2.64 (m, 16H, OCC*H*$_2$C*H*$_2$OC), 3.03 (t , J=12.78, 8H, SC*H*$_2$), 3.4-3.8 (m, 909H, OC*H*$_2$C*H2*), 4.25 (t, J= 9.05, 8H, C*H*$_2$OCO), 4.34 (t, J=21.8, 8H, C*H*$_2$OCO), 7.11 (d, J=11.8, 4H, NCC*H*), 7.58-7.68 (m, 8H, CHC*H*C*H*N), 8.45 (d, J= 4.23 Hz, 4H, C*H*N).

3.8. Synthesis of 4 arm PEG-SH (P5)

Terra-arm PEG tetra thiol (**P5**) (Mn=10425 g/mol) was synthesized according to the literature [32]. Briefly PEG (500 mg, 0.05 mmol) was dried by removal of water by azeotropic evaporation of toluene/water and left under vacuum for 18 h. Previously dried PEG was dissolved in anhydrous toluene (8 mL), and pTSA (3.4 mg, 0.02 mmol) and mercaptopropionic acid (212 mg, 2.0 mmol) mixture was added into PEG solution. Reaction mixture was refluxed for 2 days at 110^o C. Thereafter, solvent was removed under reduced pressure, and residue was precipitated in cold diethyl ether. Then, all precipitates were collected and dissolved in methanol (1 mL) and 1 meq of DTT (7.3 mg, 0.047 mmol) and 1 meq of TEA (4.8 mg, 0.047 mmol) was added. Reaction was stirred under N_2 for 5 hours. Reaction mixture was precipitated in cold diethyl ether after removal of methanol under reduced pressure. Precipitates were filtered through a sintered glass and washed with 2-propanol and then hexane. The product (**P5**) was obtained in 70% yield as a white powder with 95% end group conversion according to ^{1}H NMR analysis (Figure 4.9).

3.9. Representative Hydrogel Synthesis

Hydrogels were obtained using the thiol-disulfide exchange reaction by mixing 1 to 1 molar equivalent of thiol to disulfide ratio to make 33% (m/v) solution in PBS (7.4 pH). As a representative synthesis of 10k-HG, polymer **P5** (19.4 mg) in 70 μL PBS (7.4 pH) was added onto polymer **P3** (20 mg) dissolved in 50 μL of PBS (7.4). The mixture was vortexed immediately to get a homogeneous hydrogel. Less than 1 min later, no flow of sample was observed when Eppendorf tube was tilted. To ensure complete crosslinking of polymer chain-ends, gelation was continued for 20 h at 37 °C shaking. The resulting gel was purified by incubating in deionized water at 37 °C with gentle shaking for at least 1 h to remove non-crosslinked polymers. The aqueous media in which hydrogel was incubated was changed periodically.

For synthesis of hydrogels with FITC-dextran encapsulation, tetra-arm PEG-PDS was dissolved in FITC-dextran containing PBS and then 4-arm PEG-SH was added on PEG-PDS solution. Mixture was vortexed quickly and left for 20 h to ensure complete crosslinking. The hydrogel samples were washed gently for 10 min in 1 mL of relevant medium (PBS) with shaking to remove unloaded macromolecules before release studies. The amount of dextran in washing media was measured with UV-spectrophotometer and plotted as 0^{th} hour release. (Figure 4.25)

3.10. Swelling Studies

Freeze-dried hydrogel (10 mg) sample was transferred to a flask containing deionized water (50 mL) at room temperature. At definite time intervals, the hydrogel sample was removed from water and weighed after drying the surface absorbed water by the help of a moisturized filter paper.

3.11. Gelation Yield of Hydrogels

Gelation yield of hydrogels was calculated gravimetrically. First, hydrogel was washed with deionized water at 37 °C shaking for at least 1 h to remove non-crosslinked polymers. Washing water was changed periodically. Then, hydrogels were freeze-dried to calculate gelation yield. Dried hydrogels masses (M_{dried}) was used to calculate yield of gelation processes as (M_{dried}/M_{p+c})*100 where M_{p+c} was the total mass of polymer and crosslinker used in gelation media.

3.12. Degradation Studies

Degradation profile of hydrogels was recorded by measuring G' and G'' values of freshly prepared and pre-swelled hydrogel in the presence of 3 mL of 10 mM glutathione at 37 °C using Anton Paar MCR 302 rheometer. To avoid solvent evaporation during measurements, a solvent trap was used.

3.13. Release Studies

Fluorescein isothiocyanate (FITC) labeled Dextran (Mn=20000 g/mol and Mn=150000 g/mol) was encapsulated into hydrogels as described above. After gelation, surfaces of hydrogels were washed with 1 mL of PBS (7.4) for 10 minutes at 37 °C with shaking and washing water was replaced with 1mL of fresh PBS. Release media was replaced with 1mL fresh PBS each hour. Data were collected periodically. The amount of cumulative dextran release in the supernatant was determined by UV-vis spectroscopy.

3.14. Rheology Analysis

To investigate rheological behaviors of hydrogels Anton Paar MCR 302 rheometer was used. Amplitude swept test was applied on swollen solid state hydrogels to investigate strain amplitude dependence of their sol-gel behavior which gives an information on visco-elastic characteristics of gels. Strain sweep test gives linear-viscoelastic limit regime (LVR) which is described as the safe region for G' and G'' and undisturbed gel structure. Frequency sweep test also gives information on the behavior of gel below critical strain. A frequency independent G' value indicates more solid state of gels.

3.15. Scanning Electron Microscopy

Swollen hydrogels were freeze-dried by lyophilization overnight. Lyophilized samples were cut into little pieces in a way that allows porous structure visible by SEM. Inner structure of hydrogels was examined by using with JEOL NeoScope JCM-5000 scanning electron microscopy (SEM) instrument at an accelerating voltage of 10kV.

3.16. End Group Analysis

To investigate end group conversions of polymer precursors within the hydrogel, two methodologies were followed. First, remaining free thiol amount originating from 4-arm PEG-SH was determined by Ellman's sulfhydryl assay. Briefly, pre-washed and freeze-dried 5 mg hydrogel was immersed in 2.5 mL of PBS (pH=8) and 1 mL of stock solution containing DTNM (4 mg/mL) was added on reaction buffer. Mixture was incubated for 2 h at 37 °C. Total amount of free thiols were calculated by measuring absorbance of TNB species using molar extinction coefficient of 14 150 M^{-1} cm^{-1}, as given in literature [33].

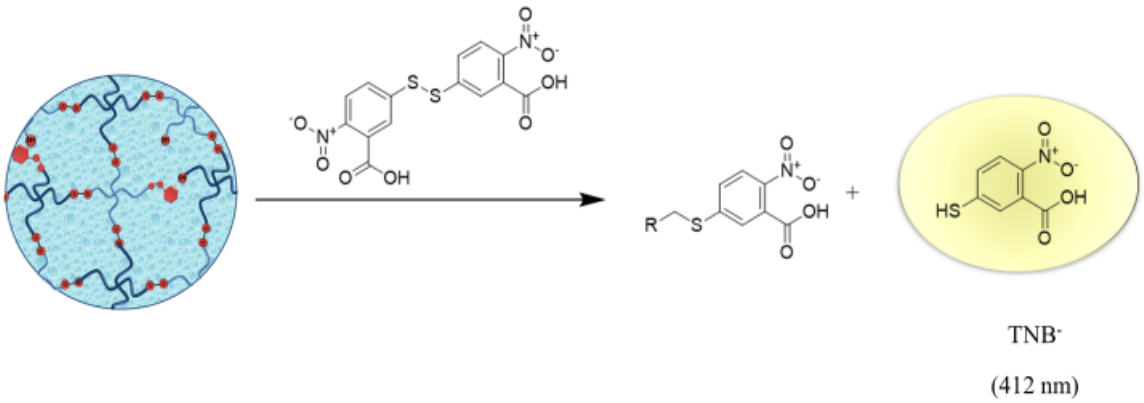

Figure 3.1. Ellman's analysis for free thiol determination.

Secondly, to calculate the amount of unreacted pyridine disulfide groups, 4-arm PEG-PDS (5 mg) pre-washed and freeze-dried hydrogel was immersed in of 10 mM DTT solution (1 mL) and incubated at 37 °C. When the hydrogel completely degraded to yield a clear solution, the absorbance of pyridine-2-thione was measured at 343 nm using a UV-spectrophotometer and its concentration was calculated using the Beer's Law [12].

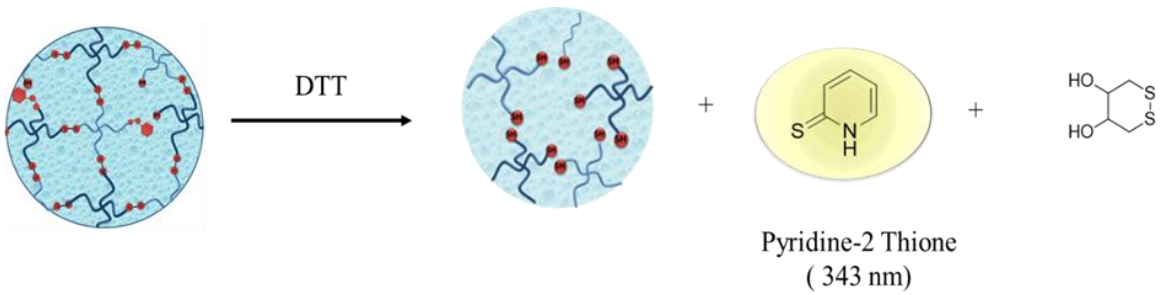

Figure 3.2. Determination of unreacted pyridine disulfide groups in hydrogels.

4. RESULTS AND DISCUSSION

4.1. Synthesis of Macromers

4.1.1. Synthesis of 4 arm PEG-COOH

The synthetic scheme of the synthesis of tetra-arm PEG-COOH is shown in Figure 4.1. It is an esterification reaction between the hydroxyl ends of PEG and succinic anhydride. By this reaction, we gain carboxylic acid functional groups to attach 2-(2-pyridinyldithio) ethanol to the tetra-arm PEG polymer via facile and effective esterification reaction. Excess amount of succinic anhydride was used to ensure maximum esterification on all four arms of PEG. End group conversion was calculated by comparing the integration of peak originating from succinic anhydride at 2.64 ppm and the peak belonging to the PEG-OCH_2CH_2 adjacent to the ester at 4.25 ppm and end group conversion was estimated as nearly 90% for the tetra-arm 10k-PEG-COOH polymer (Figure 4.2). Similar procedure was utilized to synthesize tetra-arm 20k-PEG-COOH polymer with higher amounts of reagents to facilitate the reaction. It was obtained with nearly quantitative end group conversion with high purity (Figure 4.3).

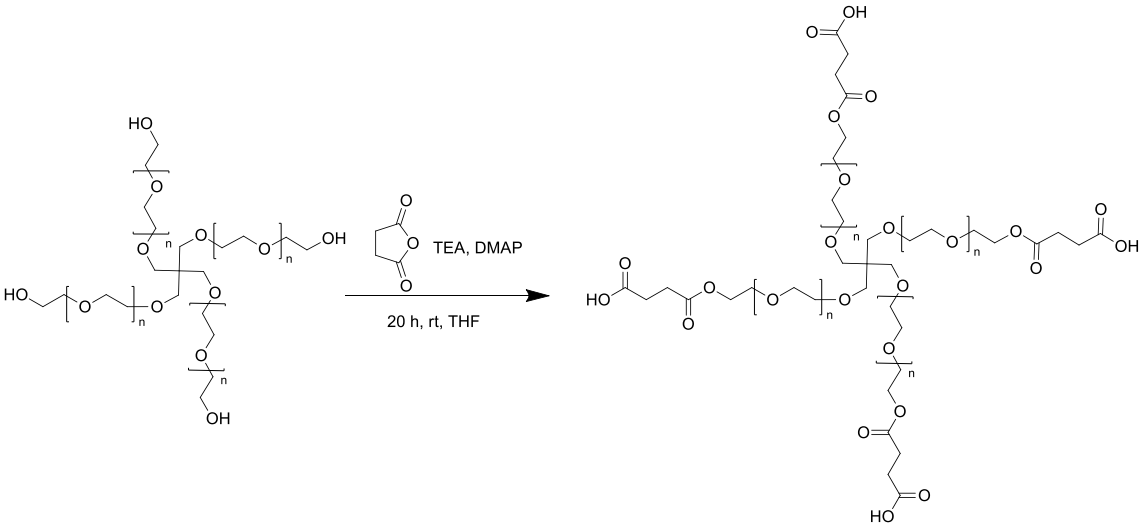

Figure 4.1. Synthesis of tetra-arm 10k-PEG-COOH polymer.

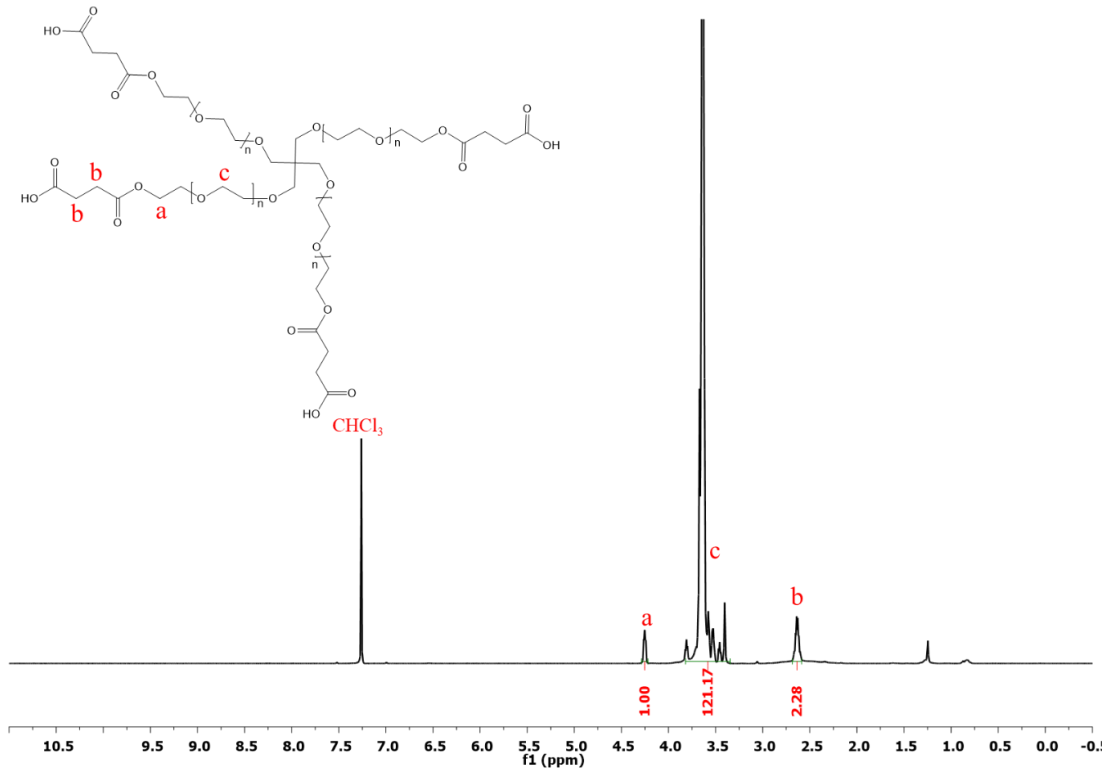

Figure 4.2. ^{1}H-NMR spectrum of tetra-arm 10K-PEG-COOH polymer.

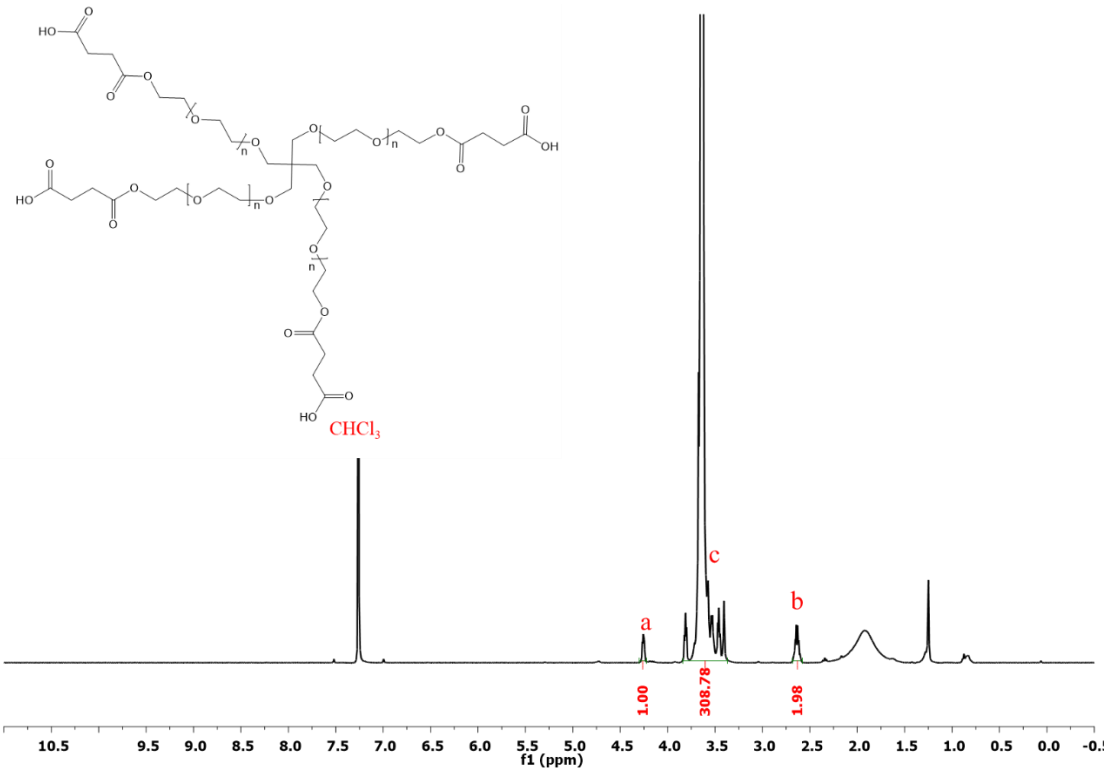

Figure 4.3. ^{1}H-NMR spectrum of tetra-arm 20k-PEG-COOH polymer.

4.1.2. Synthesis of tetra-arm PEG-PDS polymer

Crosslinked 3D network structure was planned to be achieved via thiol-disulfide exchange reaction in hydrogels. To obtain a disulfide group on polymer chain ends, a pyridine disulfide group bearing alcohol containing fragment was found suitable and synthesized according to the procedure given in literature [30]. The pyridyl disulfide group upon fragmentation releases a pyridine-2-thione fragment which is detectable using UV-Vis spectroscopy. This enables quantification of any residual PDS units within the hydrogel. This correlation sheds light on the presence of unreacted chain end i.e. crosslink defects within the hydrogels.

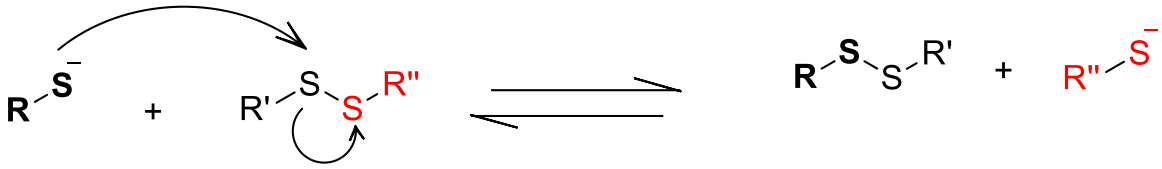

Figure 4.4. The thiol-disulfide exchange reaction.

The synthetic scheme of the synthesis of 4 arm PEG-PDS is shown in Figure 4.5. It utilizes an EDCI/DMAP coupling reaction between the carboxylic acid ends of the tetra-arm PEG-COOH and 2-(2-pyridinyldithio) ethanol. Excess amount of 2-(2-Pyridinyldithio) ethanol was used to ensure full chain end conversion of all four arms of PEG-COOH. High end group conversion (95%) was obtained for 4 arm 10k-PEG-PDS polymer as deduced from the ^{1}H NMR (Figure 4.6). Aforementioned procedure was employed to synthesize tetra-arm 20k-PEG-PDS polymer with higher equivalents of reagents to obtain high end group transformations. The 20k-PEG-PDS polymer was obtained with high end group conversion (%90) in pure form as evident from ^{1}H NMR analysis (Figure 4.7).

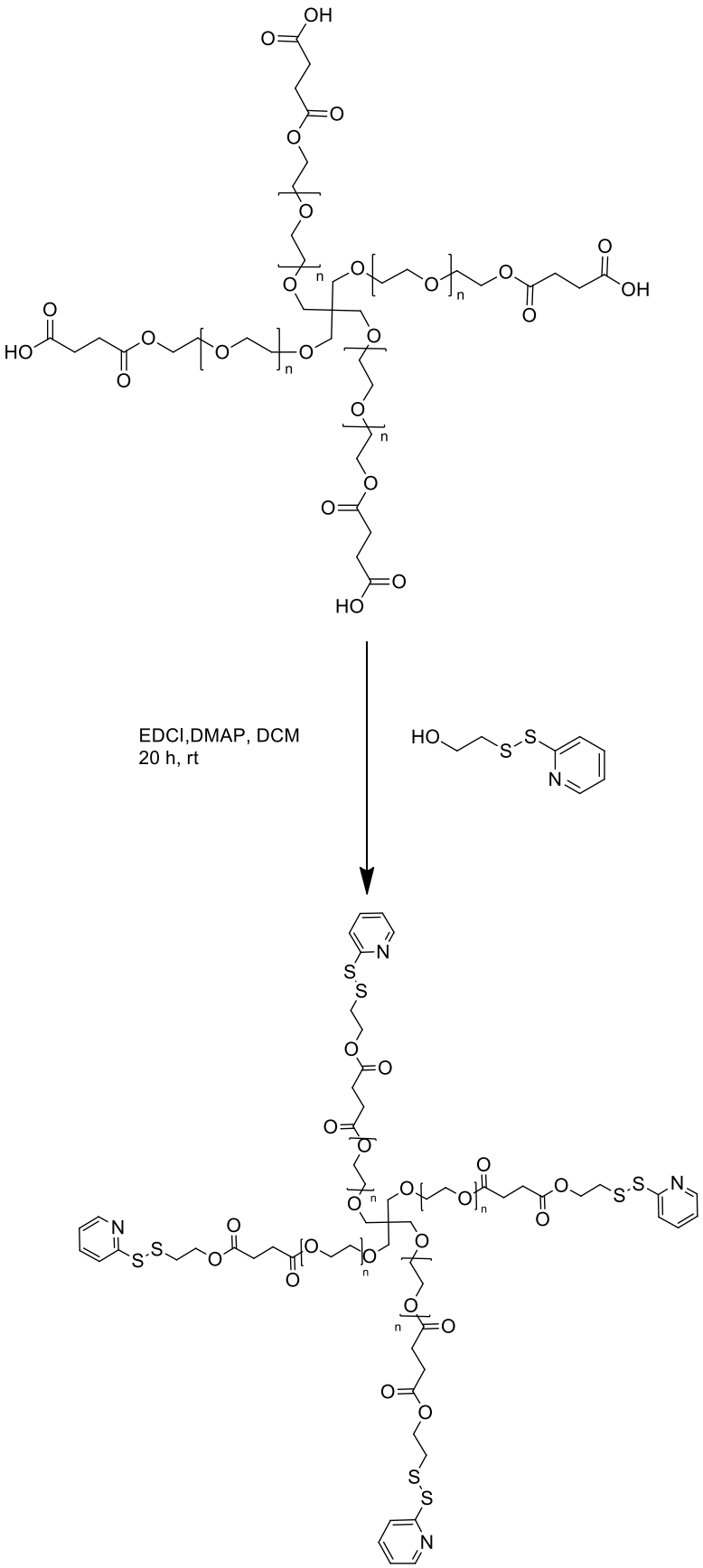

Figure 4.5. Synthesis of tetra-arm PEG-PDS polymer.

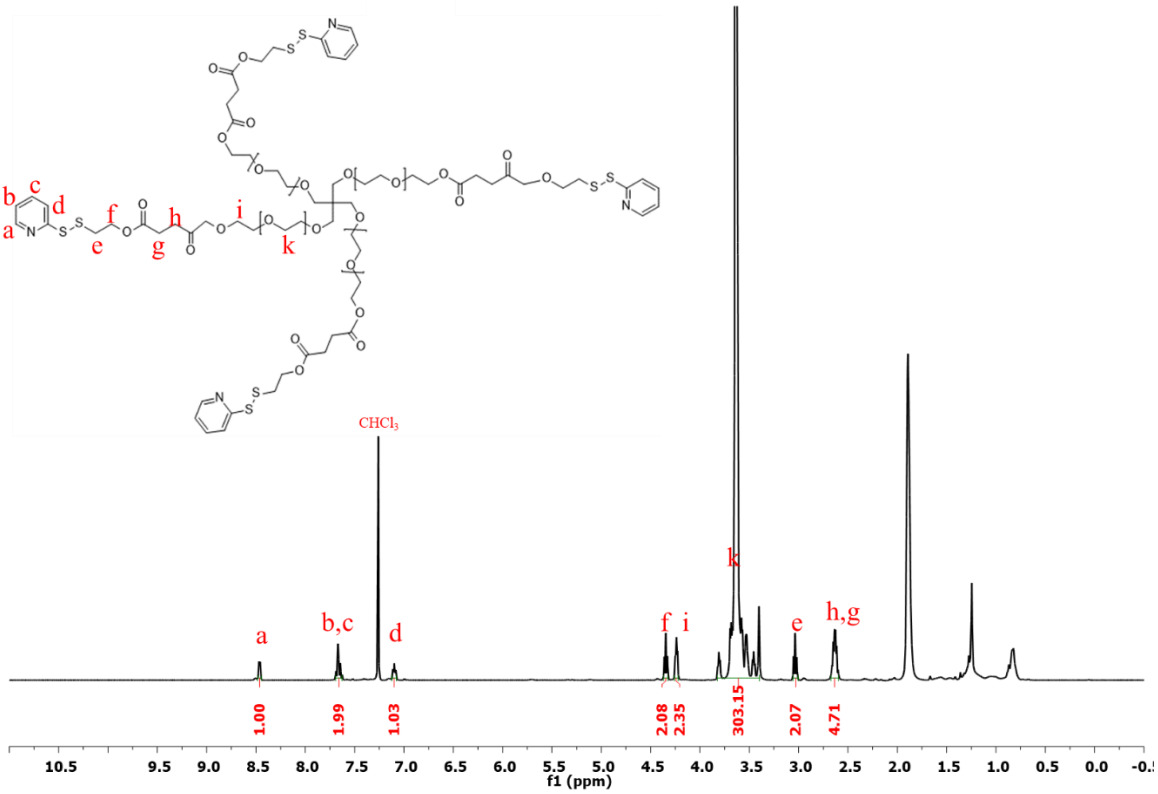

Figure 4.6. ^{1}H NMR of tetra-arm 10k-PEG-PDS polymer.

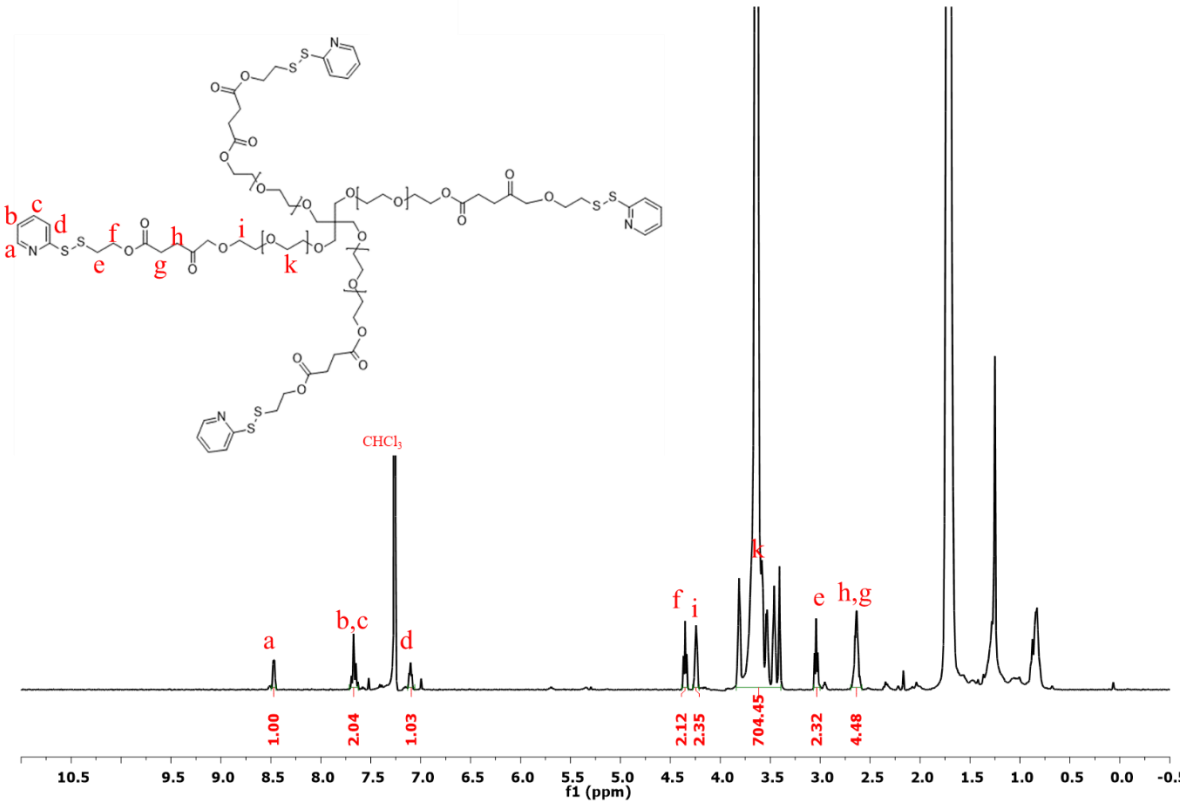

Figure 4.7. ^{1}H NMR of tetra-arm 20k-PEG-PDS polymer.

4.1.3. Synthesis of 4 arm PEG-SH

A tetra-arm PEG tetra-thiol was chosen for gelation reaction due to its high selectivity towards activated disulfide functional group bearing materials. Reaction between these species are fast and are realized with high conversions. More importantly, thiol-disulfide exchange reaction has an environment friendly nature due to metal-free and UV-free reaction conditions. To have a biomedical application potential of our hydrogels we designed this system in a way that it is minimalized to have remaining thiol species in bulk gels, which might interact with naturally occurring disulfide or thiol containing molecules in body. Additionally, well-defined inner compositions of hydrogels are preserved, allowing controlled release and selective bio-degradation.

The synthetic scheme of the synthesis of tetra-arm PEG-SH is shown in Figure 4.8. Mercaptopropionic acid is a bifunctional commercial chemical having a carboxylic acid and a thiol group. Reaction with tetra-arm PEG-OH with the carboxylic acid containing thiol is realized with the help of p-toluenesulfonoic acid as an organic catalyst. High end group conversion (95%) was obtained as deduced from ^{1}H NMR analysis (Figure 4.9).

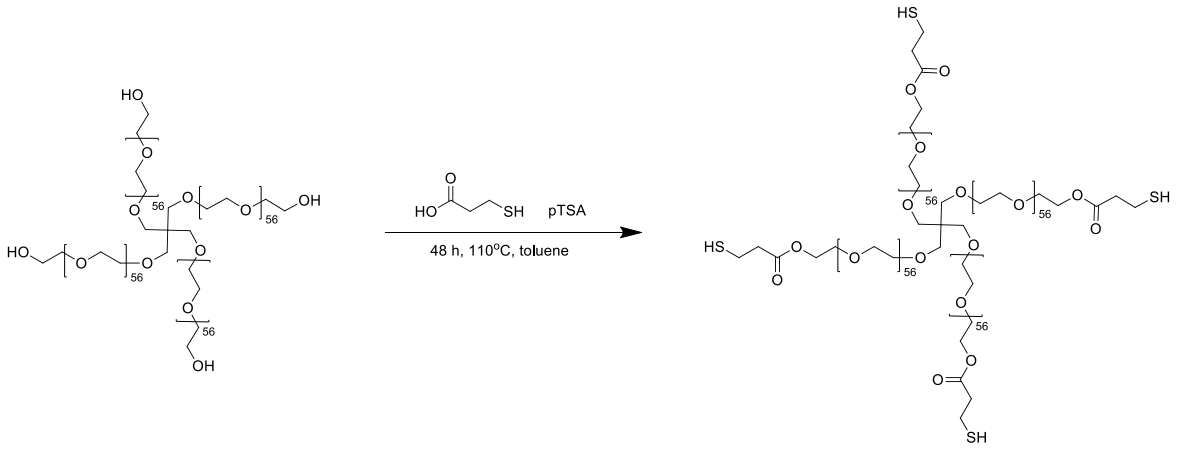

Figure 4.8. Synthesis of tetra-arm PEG-SH polymer.

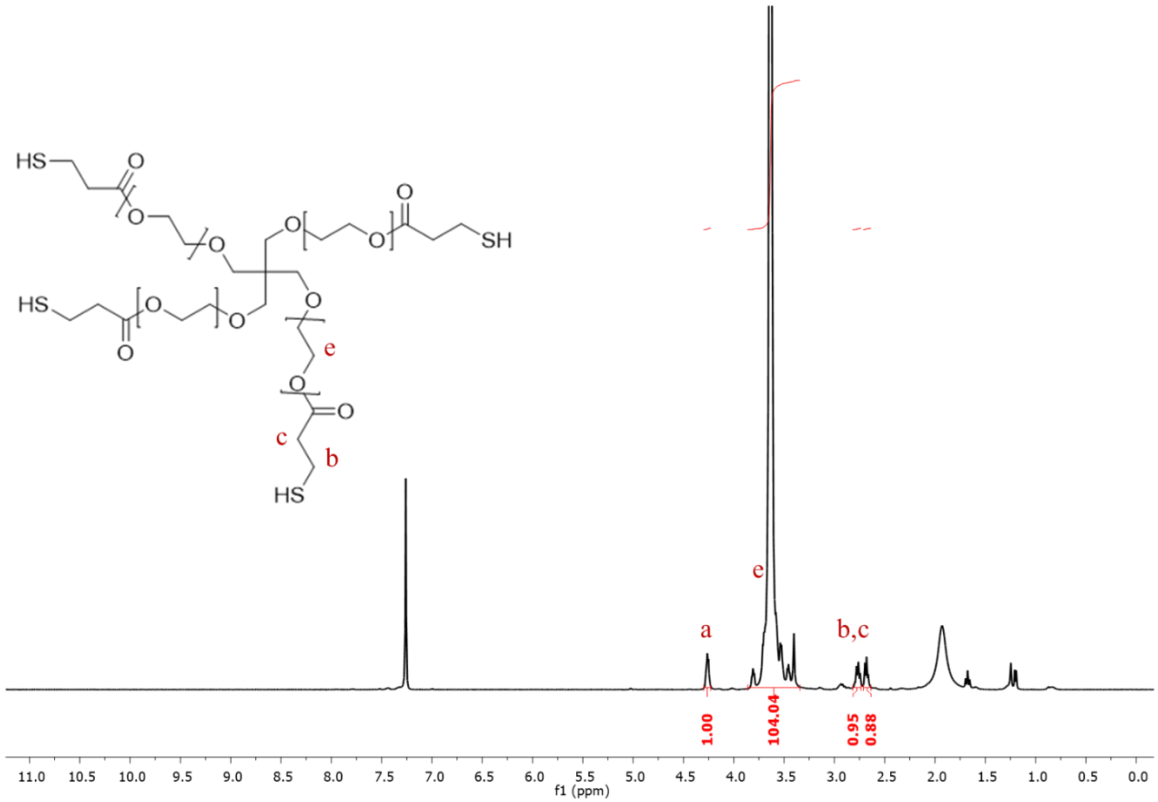

Figure 4.9. ^{1}H NMR of tetra-arm PEG-SH polymer.

4.2. Preparation and Characterization of Hydrogels

Hydrogels with varying pore sizes can be obtained by changing one of the experimental parameters such as change in the concentration of macromers, time, temperature, or by changing the chain length of reactive polymeric materials. The control over pore size leads tunable swelling capacity, visco-elastic behavior, degradation profile, and variable release profiles of small molecules from hydrogel matrix. In this project, we designed hydrogels with well-defined network structures with different pore sizes to examine loading and releasing profiles of macromolecules with different sizes by changing the molecular weight between crosslinking junction points. Thus, we attempted to keep all other variables same but vary the chain length of one of the polymeric components, namely the PEG-PDS polymer. As it can be seen from the Table 4-1, hydrogels with high conversions were obtained, as a result of effective reaction between the pyridyl disulfide and thiol groups on the hydrogel precursors.

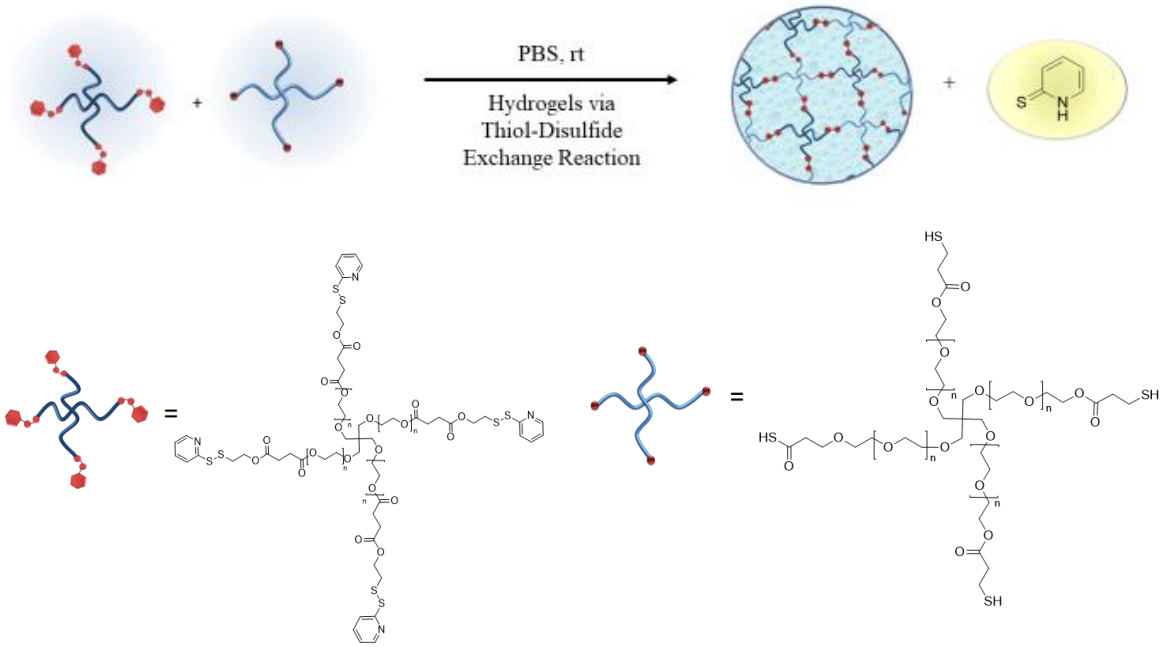

Figure 4.10. Schematic illustration of gelation mechanism of hydrogel formation.

Analysis of chemical structure of hydrogels are challenging due to their insoluble nature. A reasonable estimate about effectiveness of the chain-chain linkage formation can be obtained through analysis of the residual end-groups within the hydrogels. To determine the effectiveness of the chain-chain coupling reaction, we conducted Ellman's test to find out residual thiol groups remaining in gel matrix, which indicates amount of thiol chain ends that did not get crosslinked. Likewise, the residual pyridyl disulfide chain ends of polymers within hydrogel are estimated by their forced release from the hydrogel which results in release of these fragments as UV-active pyridinethione units. Details of these procedures are described in the experimental sections.

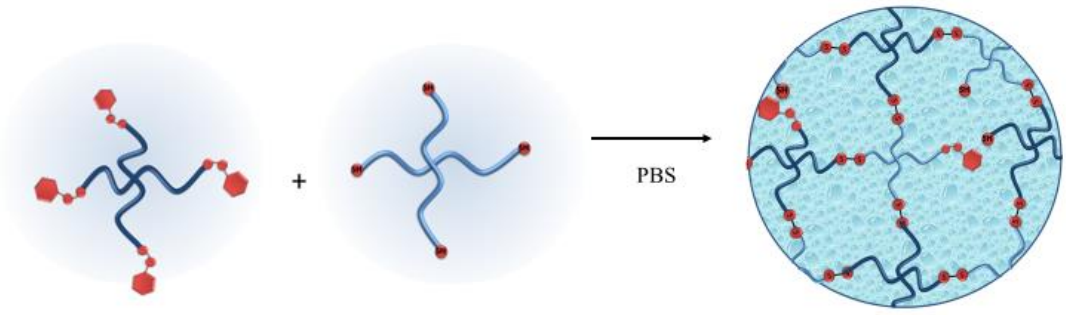

Figure 4.11. Schematic illustration of possible defects in hydrogel matrix.

The results of end group analysis of the hydrogels are summarized in the Table 4-1. Slightly lower end group conversions for the 20k-HG hydrogel can be explained by the more demanding steric hindrances encountered during the step growth mechanism of gel formation process. Gravimetric conversion of 20k-HG hydrogel is high because the reaction is fast and efficient but forming disulfide bridges all over the hydrogel matrix is difficult because of higher chain length of the polymeric precursor **P4**. On the other hand, while the gravimetric gel conversion for the 10k-HG hydrogel is almost as good as for the 20k-HG hydrogel, the end group conversion is much higher due to the shorter chain lengths of PEG polymers involved in the crosslinking process. While the hydrogels were opaque in their dry state, they became transparent upon swelling in aqueous media (Figure 4.13). Both hydrogels were obtained with highly porous structures, as deduced from the morphological analysis obtained from SEM analysis (Figure 4.13). A porous structure leads to effective swelling of hydrogels in aqueous media. Higher chain length in 20k-HG induces formation of larger pores, which in turn, resulted in higher water uptake capacity (Figure 4.14).

Figure 4.12. Photographs of hydrogels in dry and wet state.

Following the determination of their equilibrium swelling, visco-elastic properties of these hydrogels were investigated using rheologic analysis. While the sol to gel transition occurs rapidly as evident from lack of flow of the polymeric mixture within a minute of mixing, it does not indicate the extent of crosslinking within the hydrogel. The storage modulus a hydrogel is related to the efficiency of crosslinking. Hence, we prepared several hydrogels and left them to undergo gelation for different time periods, then we washed out any unreacted polymers. As expected, an increase in the storage modulus (G') of hydrogels was observed upon increasing the gelation period (Figure 4.15). As it can be observed from the frequency sweep plots, uncompleted crosslinking in early stages of gelation, results in

weak gels with lower storage modulus values. When conversion reaches its maximum efficiency, no more increase in G' is observed i.e. we see almost no difference between the modulus of gels at 25th h and 30th h in frequency sweep test.

We also have done rheological analysis on two different hydrogels (10k-HG and 20k-HG) to examine the effect of chain length between crosslinking points on physical properties of hydrogels like mechanical strength. It was observed that shorter chain length results in hydrogels with higher G' value and stiffer gels. The 20k-HG possesses G' around 1000 Pa after 20 h of gelation (Figure 4.17), while the 10k-HG obtained with the same gelation time has an almost 10 fold greater G' (Figure 4.16), at around 10 000 Pa. This stiffness of gels can be correlated to the equilibrium swelling capacity of the hydrogels. As expected, hydrogels obtained using polymers with shorter arm lengths exhibit comparatively lower swelling in water than the ones obtained using polymers with longer chains.

Table 4. 1. Library of hydrogels with different polymer chain lengths

Hydrogel	**m/v % [a]**	**Conversion %**	**Free Pyridyldisulfide %**	**Free Thiol %**	**Eq.Swelling Ratio (%)**
10k-HG	**33**	**89±1.8**	**2.9±1.3**	**1.8±1.3**	**787**
20k-HG	**33**	**93±1.6**	**13±1.6**	**3.2±0.6**	**2078**
a: mass of macromer in gel media / volume of PBS					

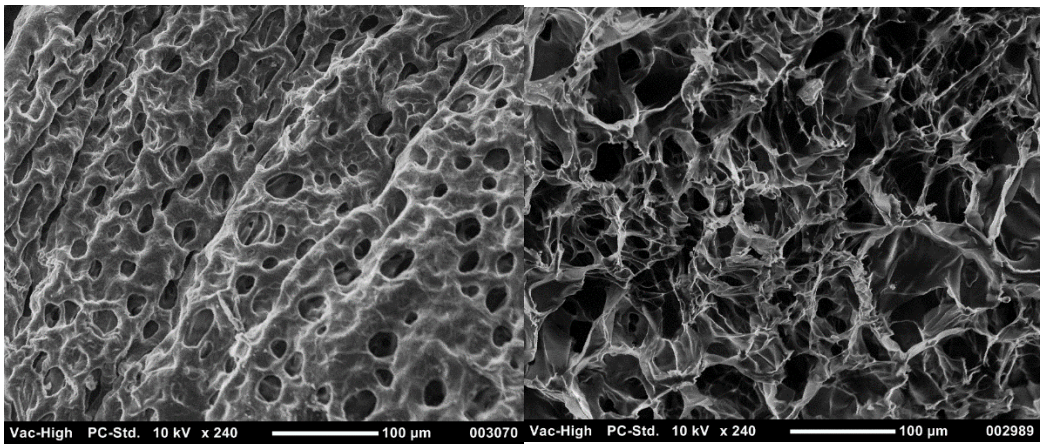

Figure 4.13. SEM micrographs of 10k-HG (left) and 20k-HG (right) hydrogels.

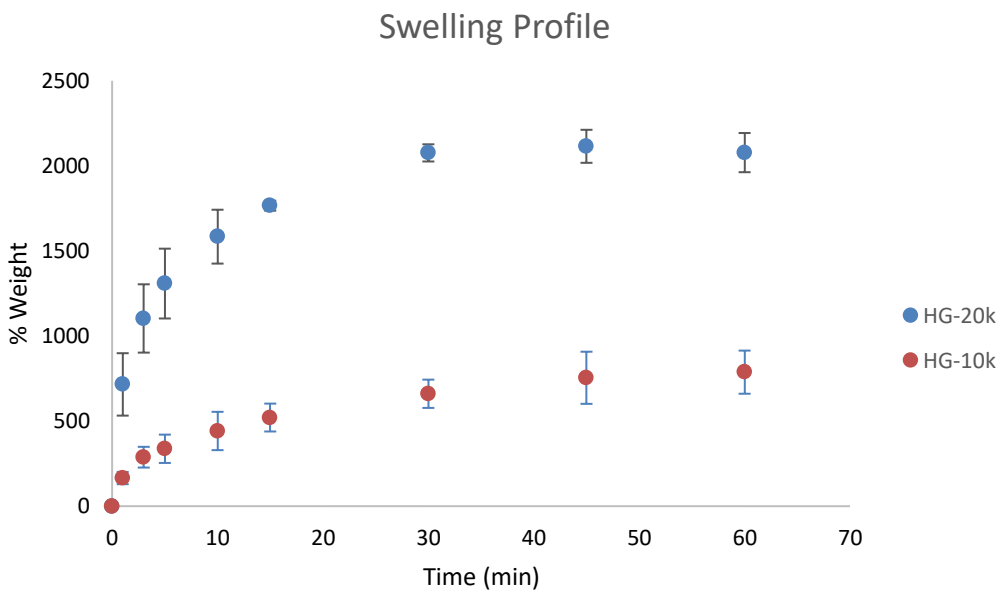

Figure 4.14. Effect of chain length on swelling capacity of hydrogels.

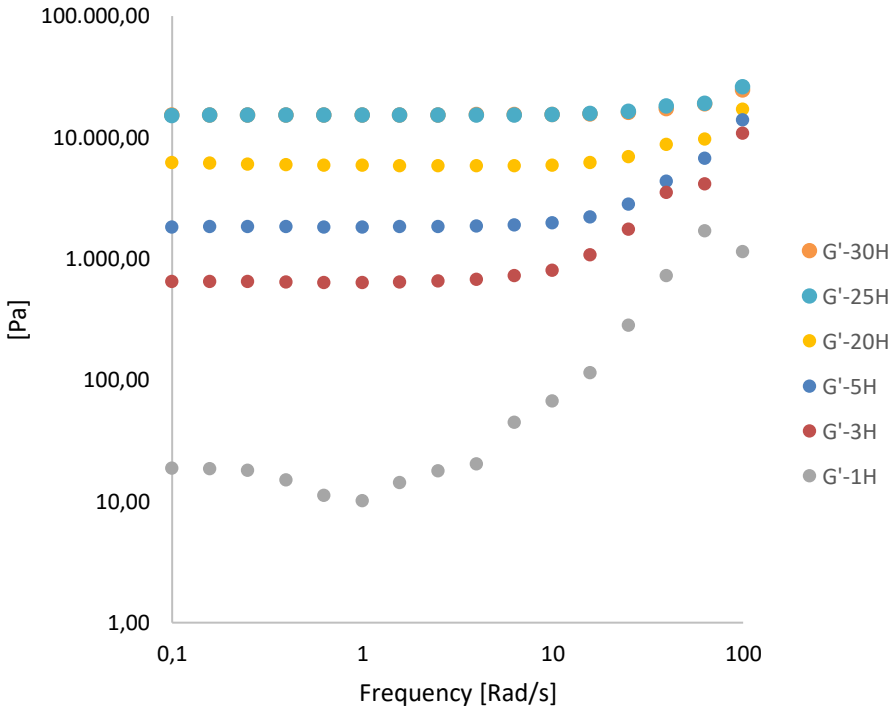

Figure 4.15. Frequency sweep test for time dependence on the storage modulus of 10k-HG.

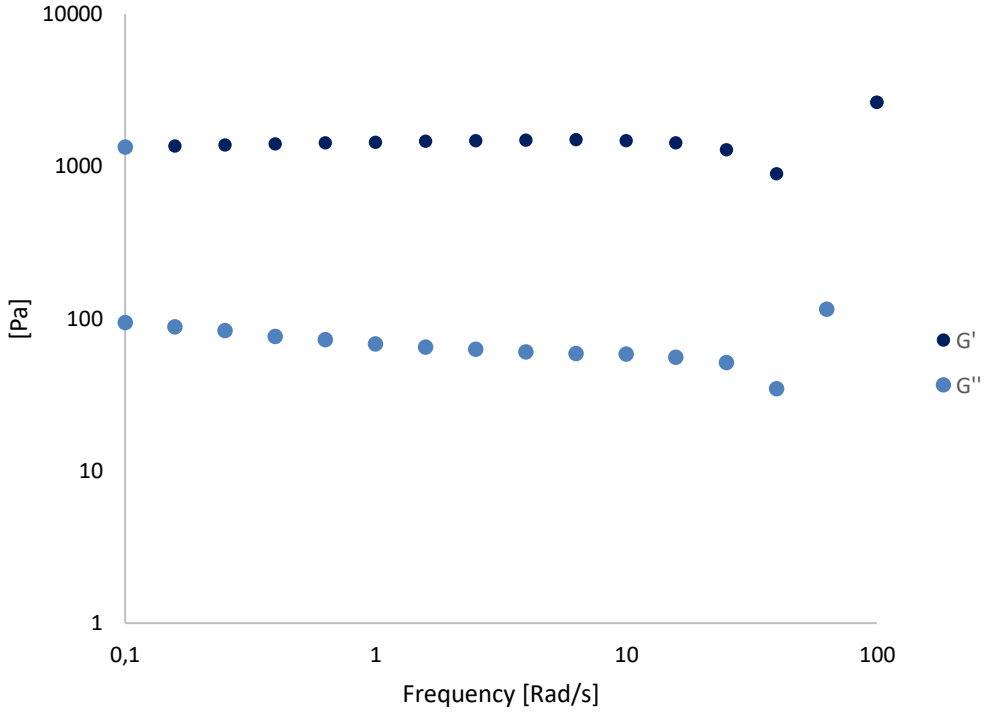

Figure 4.16. Frequency sweep test of 20k-HG at 20th hour

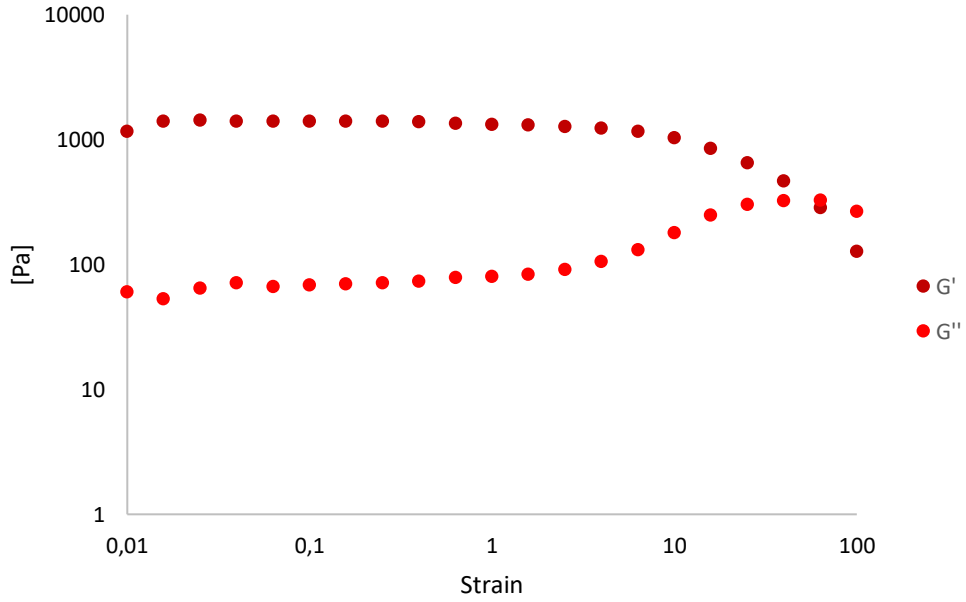

Figure 4.17. Strain sweep test of 20k-HG at 20th hour

By rheological studies, we showed that both of our gels show gel-like structure i.e. G' is higher than G'' for both. They are stable, durable, and can be suitable for biomedical applications. Rheology data also discloses the G' values of these hydrogels are in the range

observed for many tissues [34]. It should be noted that the onset of gelation was very fast. It was not possible to determine gelation point by rheologic measurements due to the fast crosslinking nature of reactive species. Gelation occurs within seconds i.e. prior to the start of rheological measurements.

4.3. Degradation of Redox Responsive Hydrogels

Hydrogels are bulk materials that can be used as a carrier for biomolecules or cells. They allow sustained release of cargo by diffusion or via stimuli responsive degradation of hydrogel network. Degradability of gel is important not only for the delivery purposes but also in terms of biocompatibility. Retention of the bulk and insoluble polymeric matter for long periods of time may have potential risks such as deformation, inflammation, and even toxicity for the tissue where the gel is implanted. Disulfide crosslinked hydrogels can undergo degradation in the presence of reduced glutathione which is a biosynthetic product of cells. They are also prone to disintegrate in the presence of other thiol containing metabolic products secreted by cells in natural tissue. Therefore, these types of gels do not require any surgery to remove the implanted material.

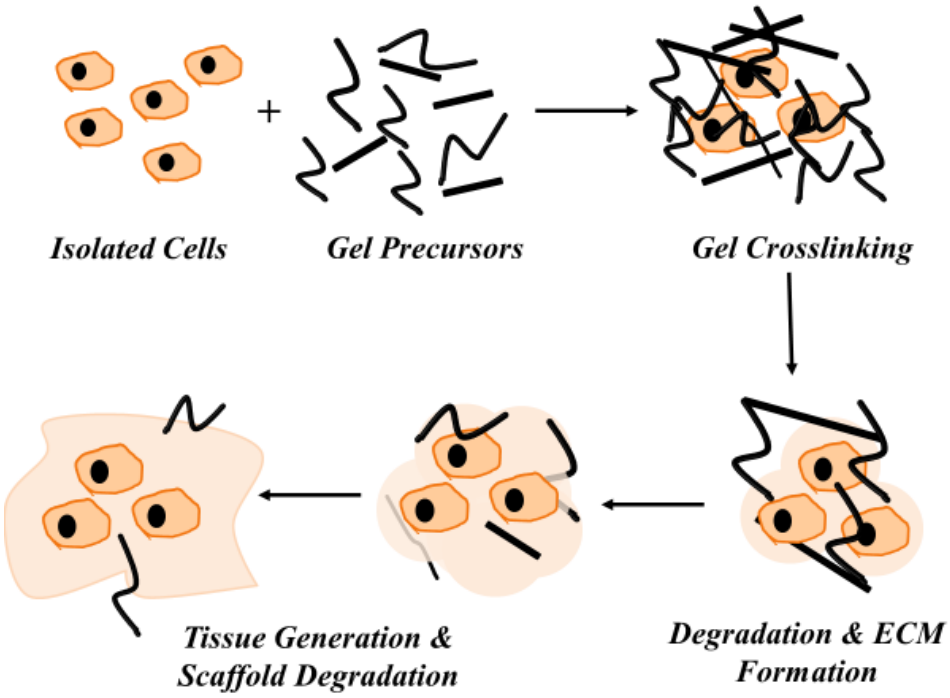

Figure 4.18. Schematic representation of cell containing gel formation, degradation and tissue regeneration for biomedical applications.

For protein and cell implantation, mesh size of hydrogel plays an important role in terms of encapsulation and retention. Cells are mostly in micron sizes, so entrapment within hydrogels are easy. But, it is crucial that the mesh size of the surrounding hydrogel be appropriate for the diffusion of nutrition, metabolic waste, and cell signaling chemicals like growth factors. As hydrogels degrade, larger pores forms and allows extra cellular matrix (ECM) proteins' diffusion for intracellular signaling, thus enabling cells to form new tissue.

For afore mentioned reasons, we aimed to obtain a cleavable network by degradation upon disulfide reduction to allow facile transport of cargo. In order to demonstrate this, degradation experiments were carried out by mimicking physiological conditions. Hydrogels were placed in rheometer at 37 °C in the presence of glutathione containing PBS (7.4 pH). Degradation was followed by following the evolution of G' and G'' values by time sweep test. A decrease in G' indicates degradation of crosslinking and dissolution of the polymeric network. The crossover point between G' and G'' suggests the transition of the gel from gel to sol form.

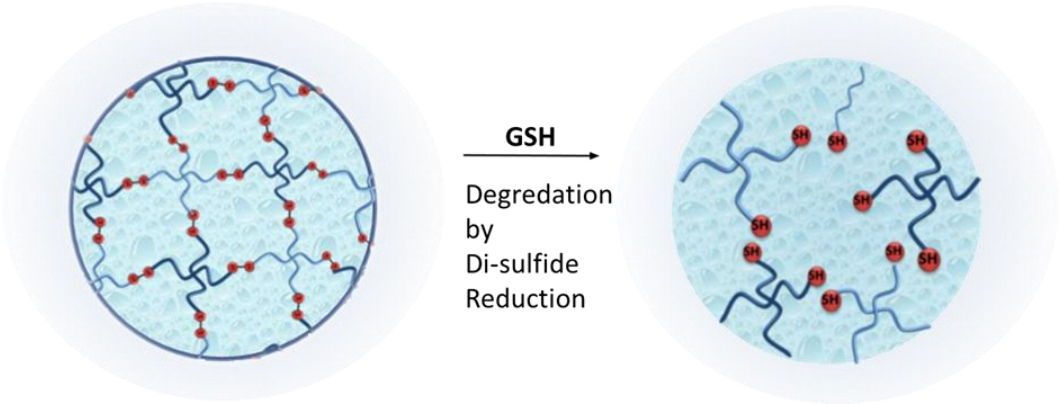

Figure 4.19. Schematic illustration of degradation of hydrogel.

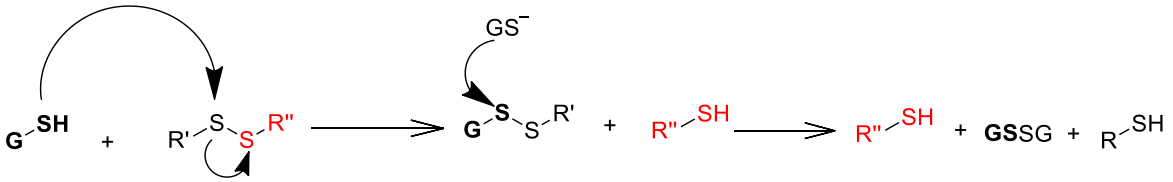

Figure 4.20. Disulfide bridge reduction via glutathione.

Rheological measurements were undertaken by treating the hydrogels swollen to their equilibrium swelling state with glutathione. As expected, a fast degradation wthin 38 min was observed for the hydrogel with the lower storage moduli i.e. 20k-HG. In comparsion, the 10k-HG hydrogel loses its integrity in the presence of the disulfide reducing agent after 3.5 h under the same conditions. Thus, physical properties of hydrogels such as their porosity, strength, and crosslinking density plays an important role on degradation profile.

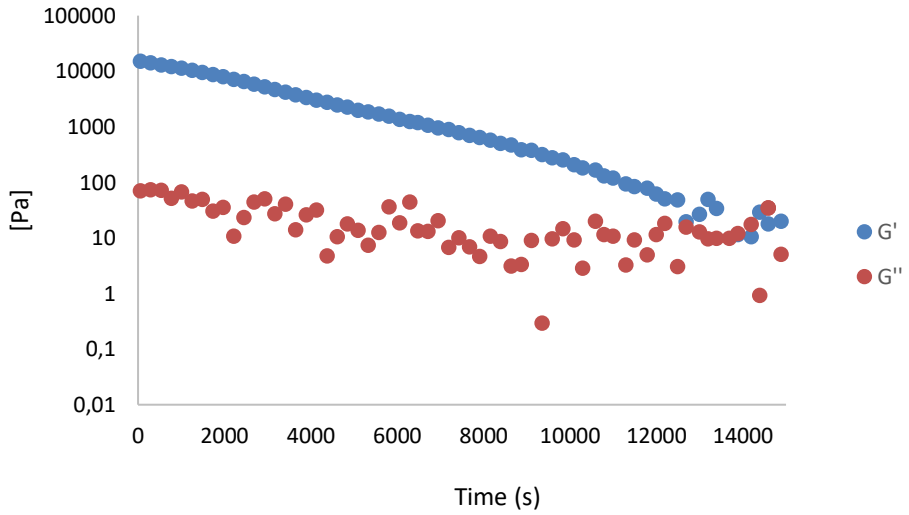

Figure 4.21. Rheological analysis of degradation process of 10k-HG hydrogel in the presence of 10mM glutathione.

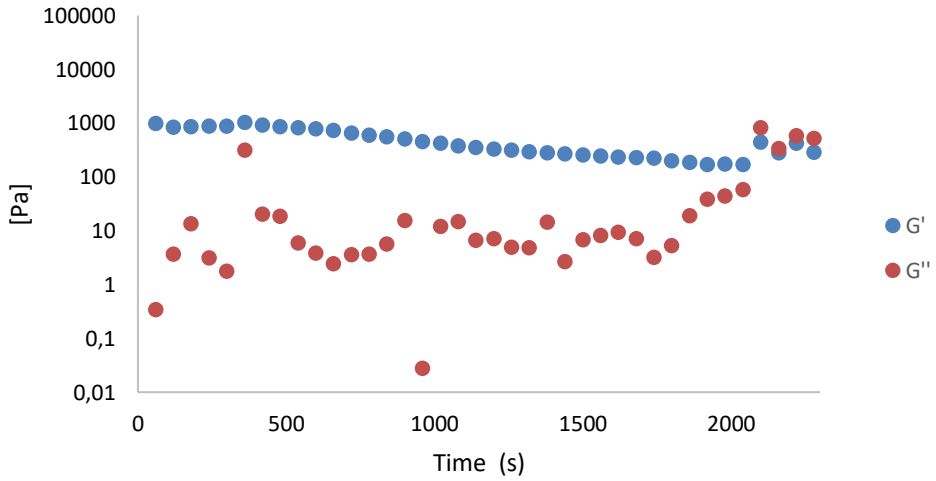

Figure 4.22. Rheological analysis of degradation process of 20k-HG hydrogel in the presence of 10mM glutathione.

4.4. Release of Macromolecules from Hydrogels

For probing the diffusion of macromolecules such as model proteins from obtained hydrogels, a fluorescent dye labeled polymer FITC-Dextran was used. Dextran is a water soluble polysaccharide that contains glucose units joined together via glucoside linkers. Various molecular weights of dextran bearing a fluorescent dye like fluorescein isothiocyanate (FITC) are commercially available. It is facile to monitor the release of dye labeled cargo from hydrogels using simple analytical technique like UV-Vis spectroscopy. FITC-Dextran polymer was entrapped into hydrogel matrix during their synthesis by dissolving the tetra-arm PEG-PDS polymer in a stock solution of dextran and undertaking hydrogel formation by the addition of tetra-arm PEG-SH polymer. Gentle rinsing of the hydrogel with water at ambient temperature removes any loosely surface adhered dye labeled molecules.

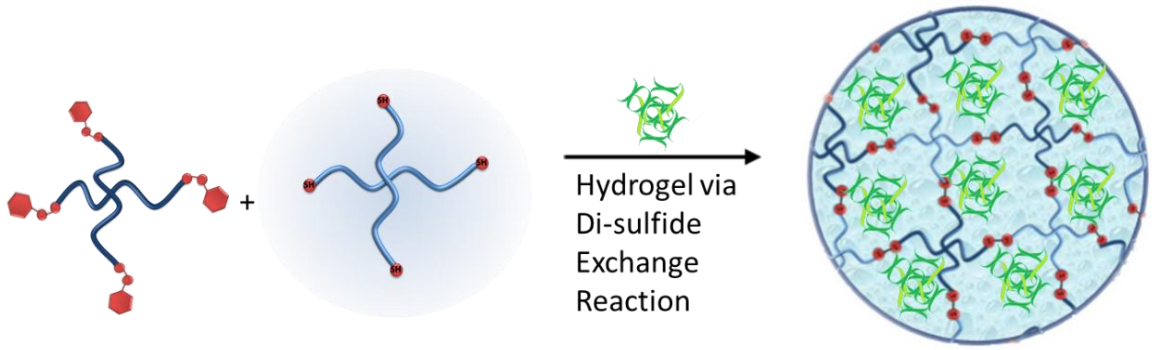

Figure 4.23. Schematic illustration of protein encapsulation in hydrogels.

Release profile of the encapsulated macromolecule is affected by degree of crosslinking, homogeneity of mesh distribution, and size of meshes through which it diffuses. Therefore, to obtain a controlled release and avoid burst release, control over the inner structure of hydrogels is needed [35]. Hydrogels with well-defined network structures ideally contain a homogeneous mesh with evenly distributed crosslinked junctions throughout the gel matrix.

Release of cargo can occur in two ways; by diffusion or by the erosion of the gel matrix. Diffusion allows the release of particles with sizes smaller than the pore size of hydrogel. On the other hand, degradation widens the pore size of gel and allows large

molecules to diffuse from gel matrix. In our design, gel starts losing its well-defined network structure through chain scission in the presence of a thiol-containing reducing agent like glutathione or DTT.

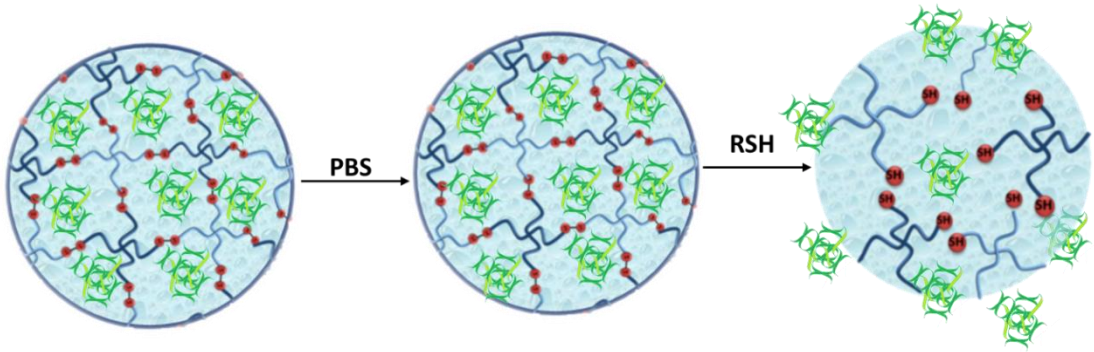

Figure 4.24. Schematic illustration of protein release from hydrogels.

In our study, freshly prepared dextran encapsulated hydrogels were rinsed with 1 mL of PBS (7.4 pH) to remove macromolecules loosely attached to their surface. The absorbance of this wash solvent was measured using a UV-Vis spectrophotometer. In order to probe the release of the dye-labeled macromolecules from the hydrogels, samples were immersed in a PBS release medium. For the following 8 hours, release media was replaced with a fresh release media every hour. After 24 h, 1 mL of 10 mM DTT was added on the gels to induce complete release. Gels degraded within minutes in the 10 mM DTT solution. The absorbance of the clear solution was measured. Using this data from the fully induced release, the % cumulative release of dextran over time was calculated.

Release of the encapsulated macromolecules with 20 kDa molecular weight from 10k-HG over 24 h in PBS was fast and high by passive diffusion. However, 150 kDa diffused out slower and less. This selectivity in terms of size of encapsulated molecule is achieved thanks to the homogenous inner structure of gel matrix design as near-ideal. Under forced release through exposure to 10 mM DTT, 100% release could be achieved. This indicates that while a sustained release can be observed under neutral conditions, a forced on-demand release can be induced at any time.

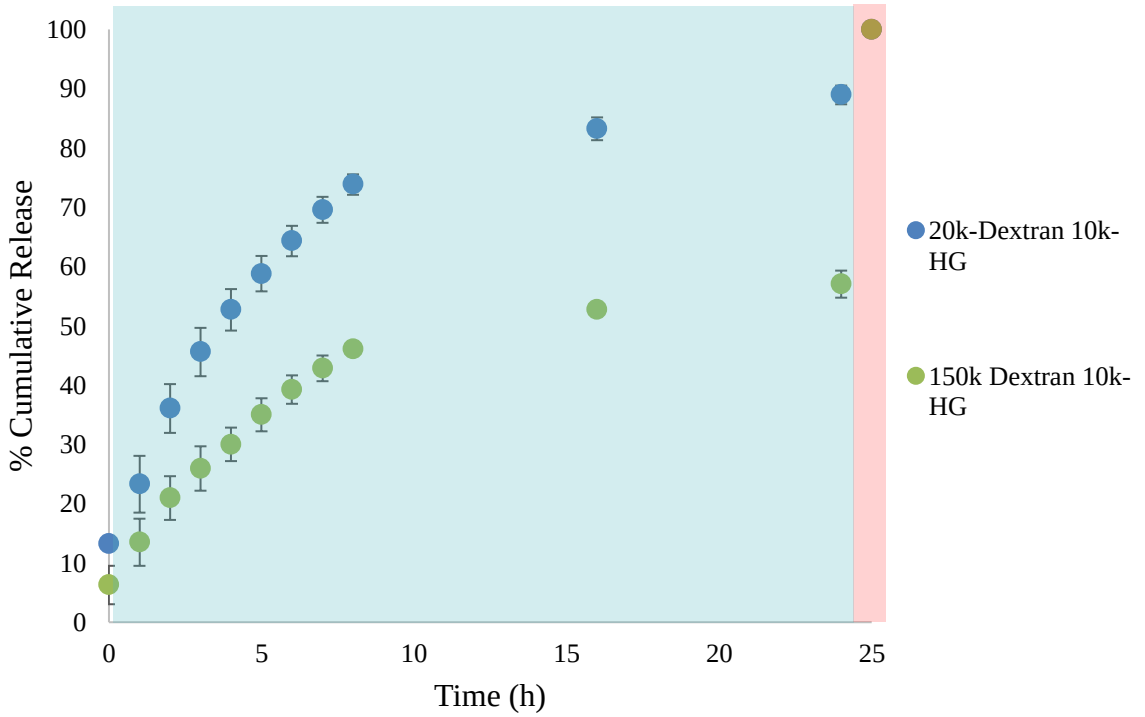

Figure 4.25. FITC-Labeled dextran release from hydrogels in PBS (7.4) for 24 h. Release in 10mM DTT at 25th h.

Hydrodynamic radius of various FITC-dextrans can be found in the literature. A table showing the ones related to our samples can be found below (Figure 4.26). According to the table, it can be concluded that the radius of dextran increasing with an increase in their molecular weight. Hydrodynamic radius of dextran molecules can provide us reasoning in terms of leakage of these molecules from hydrogel matrix. Release profile of macromolecules with two different hydrodynamic sizes were compared for 10k-HG. The slower release of the 150 kDa dextran compared to the 20 kDa dextran in PBS indicates that permeability of macromolecules within hydrogels decrease with increasing molecular weight and size [36]. Also, as observed, upon addition of DTT, the hydrogel network structure breaks down due to chain scission by breakage of disulfide linkages thus leading to fast dextran release.

Tracer	Molecular Weight (D)	Molecular Radius (nm)	Permeability Coefficient ($\times 10^{-6}$ cm/sec, mean ± SD)
Sodium fluorescein	376	0.5	84.5 ± 16.1
FITC-D, 4 kD	4,400	1.3	25.2 ± 5.1
FITC-D, 20 kD	19,600	3.2	6.79 ± 4.18
FITC-D, 40 kD	38,900	4.5	2.79 ± 1.58
FITC–BSA	67,000	3.62	5.49 ± 2.12
Rhodamine D, 70 kD	70,000	6.4	1.35 ± 0.77
FITC-D, 70 kD	71,200	6.4	1.39 ± 0.88
FITC–IgG	150,000	5.23	4.61 ± 2.17
FITC-D, 150 kD	150,000	8.25	1.34 ± 0.88

Figure 4.26. Radius of FITC-Dextrans [36].

According to SEM images (Figure 4.13), we can deduce an empirical pore size comparison of 10k-HG and 20k-H. Yet, in order to deduce a better understanding of the correlation of the mesh size with the diffusion of macromolecules, calculation of the mesh size of hydrogel using swelling and rheological measurements was necessary. As described by Kloxin and coworkers, it is possible to estimate the mesh size of a hydrogel if the average molecular weight between crosslinking joints can be calculated by the formula given below [37]. The formula below shows the relationship between shear modulus, equilibrium swelling, and molecular weight between crosslinking points.

$$G = \frac{\rho RT}{\overline{M}_c}\left(1 - \frac{2\overline{M}_c}{\overline{M}_n}\right)\left(\frac{\nu_{2,s}}{\nu_{2,r}}\right)^{1/3}$$

Using the molecular weight between crosslinking points, the mesh size can be determined by the formula given below:

$$\xi = \nu_{2,s}^{-1/3} l \sqrt{\frac{2C_n\overline{M}_c}{M_r}}$$

The table showing our calculations for 10k-HG and 20k-HG can be found below (Table 4.2).

A mesh size of 11 and 18 nm was obtained for 10k-HG and 20k-HG hydrogels, respectively. Since the mesh size in both hydrogels are quite large compared to the size of the 20 kDa FITC-dextran polymer which has a hydrodynamic radius of 3.2 nm, it corroborates that the small molecule can diffuse out in a sustained way in the absence of any external stimuli and burst release can be achieved on-demand.

Whereas, the 150 kDa FITC-dextran which has a size of 8.3 nm, closer to the mesh size of the 10k-HG, shows, as expected, a notably slower release than the former hydrogel. And its stimuli responsive forced release is shown in Figure A.2. indicating instant release can be achieved any time upon the addition of a disulfide reducing agent.

While these polymer weights were chosen as model representations for bio-related applications, for further applications, the range of polymer weight can be employed depending on the desired release profile of the biopharmaceutical agent.

Table 4. 2. Effect of polymer chain on equilibrium swelling ratio, shear modulus, average molecular weight between crosslinking points, and estimated mesh size.

Hydrogel	**Mc (g/mol)**	**Mesh Size(nm)**	**G (Pa)**	**Eq. Swelling Ratio (%)**
10k-HG	4823	11	15000	787
20k-HG	7488	18	1000	2078

5. CONCLUSIONS

In this thesis, hydrogels bearing well-defined network structures were synthesized using disulfide and thiol bearing tetra-arm PEG polymers with two different molecular weights. The fast and facile reaction between the disulfide and thiol functional groups on chain end of the polymeric reactants result in formation of hydrogels with high conversions (> 90%). The storage modulus (G') and loss modulus (G'') of hydrogels obtained using polymers with different chain lengths were recorded from rheologic measurements. The homogeneous and porous morphology of the hydrogels in their dry state was obtained using scanning electron microscopy. The water uptake capacities of hydrogels were studied by swelling test. Degradability in response to thiol-containing molecules was ensured by incorporation of disulfide linkages at the crosslinking points. Stimuli sensitive degradation was observed in the presence of reduced glutathione at 37 °C, and demonstrated using rheological measurements. Two different hydrogels with varying mesh sizes were fabricated by employing polymers with different molecular weight. Release of dye-labeled macromolecules as model proteins from these gel matrices in physiological conditions were undertaken to demonstrate that control over diffusion can be achieved by varying the mesh sizes.

REFERENCES

1. Wallmersperger, T., B. Kröplin, and R. W. Gülch, "Coupled chemo-electro-mechanical formulation for ionic polymer gels—numerical and experimental investigations", *Mech. Mater.*, Vol. 36, No. 5–6, pp. 411–420, May 2004.
2. Li, J., "Self-assembled supramolecular hydrogels based on polymer–cyclodextrin inclusion complexes for drug delivery", *NPG Asia Mater.*, Vol. 2, No. 3, pp. 112–118, July. 2010.
3. Fu, S., H. Dong, X. Deng, R. Zhuo, and Z. Zhong, "Injectable hyaluronic acid/poly(ethylene glycol) hydrogels crosslinked via strain-promoted azide-alkyne cycloaddition click reaction", *Carbohydr. Polym.*, Vol. 169, pp. 332–340, 2017.
4. Fu, S., H. Dong, X. Deng, R. Zhuo, and Z. Zhong, "Injectable hyaluronic acid/poly(ethylene glycol) hydrogels crosslinked via strain-promoted azide-alkyne cycloaddition click reaction", *Carbohydr. Polym.*, Vol. 169, pp. 332–340, August. 2017.
5. Zhang, J. and N. A. Peppas, "Synthesis and Characterization of pH- and Temperature-Sensitive Poly(methacrylic acid)/Poly(N -isopropylacrylamide) Interpenetrating Polymeric Networks", *Macromolecules*, Vol. 33, No. 1, pp. 102–107, January. 2000.
6. Han, C. K. and Y. H. Bae, "Inverse thermally-reversible gelation of aqueous N-isopropylacrylamide copolymer solutions", *Polymer (Guildf).*, 1998.
7. Kharkar, P. M., K. L. Kiick, and A. M. Kloxin, "Designing degradable hydrogels for orthogonal control of cell microenvironments", *Chem. Soc. Rev.*, Vol. 42, No. 17, pp. 7335–7372, 2013.
8. Mahinroosta, M., Z. Jomeh Farsangi, A. Allahverdi, and Z. Shakoori, "Hydrogels as intelligent materials: A brief review of synthesis, properties and applications", *Mater. Today Chem.*, Vol. 8, pp. 42–55, 2018.
9. Wang, Y., N. Yang, D. Wang, Y. He, L. Chen, and Y. Zhao, "Poly (MAH-β-cyclodextrin-co-NIPAAm) hydrogels with drug hosting and thermo/pH-sensitive for controlled drug release", *Polym. Degrad. Stab.*, Vol. 147, No. November 2017, pp. 123–131, 2018.
10. Hoffman, A. S., "Hydrogels for biomedical applications", *Adv. Drug Deliv. Rev.*,

Vol. 64, pp. 18–23, December. 2012.

11. Huglin, M. R., "Hydrogels in medicine and pharmacy Edited by N. A. Peppas, CRC Press Inc., Boca Raton, Florida, 1986 (Vol. l), 1987 (Vols 2 and 3). Vol. 1 Fundamentals, pp. vii + 180, £72.00, ISBN 0-8493-5546-X; Vol. 2 Polymers, pp. vii + 171, £72.00, ISBN 0-8493-5547-8; Vol. 3 Properties and Applications, pp. vii + 195, £8000, ISBN 0-8493-5548-6", *Br. Polym. J.*, Vol. 21, No. 2, pp. 184–184, January. 1989.
12. Matopat, *Matopat en*., http://en.matopat-global.com/our-solutions-view/wound-treatment/, accessed at November 2018.
13. Koehler, J., F. P. Brandl, and A. M. Goepferich, "Hydrogel wound dressings for bioactive treatment of acute and chronic wounds", *Eur. Polym. J.*, Vol. 100, No. January, pp. 1–11, 2018.
14. Kar, M., Y. R. Vernon Shih, D. O. Velez, P. Cabrales, and S. Varghese, "Poly(ethylene glycol) hydrogels with cell cleavable groups for autonomous cell delivery", *Biomaterials*, Vol. 77, pp. 186–197, 2016.
15. Aimetti, A. A., A. J. Machen, and K. S. Anseth, "Poly(ethylene glycol) hydrogels formed by thiol-ene photopolymerization for enzyme-responsive protein delivery", *Biomaterials*, Vol. 30, No. 30, pp. 6048–6054, 2009.
16. Fonseca, K. B., D. B. Gomes, K. Lee, S. G. Santos, A. Sousa, E. A. Silva, D. J. Mooney, P. L. Granja, and C. C. Barrias, "Injectable MMP-Sensitive Alginate Hydrogels as hMSC Delivery Systems", *Biomacromolecules*, Vol. 15, No. 1, pp. 380–390, January. 2014.
17. Navarro-Requena, C., J. D. Weaver, A. Y. Clark, D. A. Clift, S. Pérez-Amodio, Ó. Castaño, D. W. Zhou, A. J. García, and E. Engel, "PEG hydrogel containing calcium-releasing particles and mesenchymal stromal cells promote vessel maturation", *Acta Biomater.*, Vol. 67, pp. 53–65, 2017.
18. Yu, J., F. Chen, X. Wang, N. Dong, C. Lu, G. Yang, and Z. Chen, "Synthesis and characterization of MMP degradable and maleimide cross-linked PEG hydrogels for tissue engineering scaffolds", *Polym. Degrad. Stab.*, Vol. 133, pp. 312–320, November. 2016.
19. Phelps, E. A., N. O. Enemchukwu, V. F. Fiore, J. C. Sy, N. Murthy, T. A. Sulchek, T. H. Barker, and A. J. García, "Maleimide cross-linked bioactive PEG hydrogel exhibits improved reaction kinetics and cross-linking for cell encapsulation and in

situ delivery", *Adv. Mater.*, Vol. 24, No. 1, pp. 64–70, 2012.

20. Choh, S. Y., D. Cross, and C. Wang, "Facile synthesis and characterization of disulfide-cross-linked hyaluronic acid hydrogels for protein delivery and cell encapsulation", *Biomacromolecules*, Vol. 12, No. 4, pp. 1126–1136, 2011.
21. P. Martens, K. S. A., "M_Characterization of hydrogels formed from acrylate modified poly(vinyl alcohol) macromers.pdf", Vol. 41, pp. 7715–7722, 2000.
22. Lin-Gibson, S., R. L. Jones, N. R. Washburn, and F. Horkay, "Structure-property relationships of photopolymerizable poly(ethylene glycol) dimethacrylate hydrogels", *Macromolecules*, Vol. 38, No. 7, pp. 2897–2902, 2005.
23. Malkoch, M., R. Vestberg, N. Gupta, L. Mespouille, P. Dubois, A. F. Mason, J. L. Hedrick, Q. Liao, C. W. Frank, K. Kingsbury, and C. J. Hawker, "Synthesis of well-defined hydrogel networks using Click chemistry", *Chem. Commun.*, No. 26, pp. 2774–2776, 2006.
24. Liu, S. Q., P. L. Rachel Ee, C. Y. Ke, J. L. Hedrick, and Y. Y. Yang, "Biodegradable poly(ethylene glycol)–peptide hydrogels with well-defined structure and properties for cell delivery", *Biomaterials*, Vol. 30, No. 8, pp. 1453–1461, March. 2009.
25. Arslan, M., D. Aydin, A. Degirmenci, A. Sanyal, and R. Sanyal, "Embedding well-defined responsive hydrogels with nanocontainers: Tunable materials from telechelic polymers and cyclodextrins", *ACS Omega*, Vol. 2, No. 10, pp. 6658–6667, Octobar. 2017.
26. Koo, A. N., H. J. Lee, S. E. Kim, J. H. Chang, C. Park, C. Kim, J. H. Park, and S. C. Lee, "Disulfide-cross-linked PEG-poly(amino acid)s copolymer micelles for glutathione-mediated intracellular drug delivery", *Chem. Commun.*, Vol. 0, No. 48, p. 6570, December. 2008.
27. Zhang, J., A. Skardal, and G. D. Prestwich, "Engineered extracellular matrices with cleavable crosslinkers for cell expansion and easy cell recovery", *Biomaterials*, Vol. 29, No. 34, pp. 4521–4531, December. 2008.
28. Anumolu, S. N. S., A. R. Menjoge, M. Deshmukh, D. Gerecke, S. Stein, J. Laskin, and P. J. Sinko, "Doxycycline hydrogels with reversible disulfide crosslinks for dermal wound healing of mustard injuries", *Biomaterials*, Vol. 32, No. 4, pp. 1204–1217, 2011.
29. Yu, H., Y. Wang, H. Yang, K. Peng, and X. Zhang, "Injectable self-healing

hydrogels formed via thiol/disulfide exchange of thiol functionalized F127 and dithiolane modified PEG", *J. Mater. Chem. B*, Vol. 5, No. 22, pp. 4121–4127, 2017.

30. Suhrit Ghosh, and Subhadeep Basu, and S. Thayumanavan*, "Simultaneous and Reversible Functionalization of Copolymers for Biological Applications†", 2006.
31. Kharkar, P. M., A. M. Kloxin, and K. L. Kiick, "Dually degradable click hydrogels for controlled degradation and protein release", *J. Mater. Chem. B*, Vol. 2, No. 34, pp. 5511–5521, 2014.
32. Baldwin, A. D., K. G. Robinson, J. L. Militar, C. D. Derby, K. L. Kiick, and R. E. Akins, "In situ crosslinkable heparin-containing poly (ethylene glycol) hydrogels for sustained anticoagulant release", pp. 2106–2118, 2012.
33. Arslan, M., D. Aydin, A. Degirmenci, A. Sanyal, and R. Sanyal, "Embedding well-defined responsive hydrogels with nanocontainers: Tunable materials from telechelic polymers and cyclodextrins", *ACS Omega*, Vol. 2, No. 10, pp. 6658–6667, 2017.
34. Wells, R. G., "Tissue mechanics and fibrosis.", *Biochim. Biophys. Acta*, Vol. 1832, No. 7, pp. 884–90, July. 2013.
35. Leijten, J., J. Seo, K. Yue, G. T. Santiago, A. Tamayol, G. U. Ruiz-esparza, S. Ryon, and R. Shari, "Spatially and temporally controlled hydrogels for tissue engineering", Vol. 119, pp. 1–35, 2017.
36. Ambati, J., C. S. Canakis, J. W. Miller, E. S. Gragoudas, A. Edwards, D. J. Weissgold, I. Kim, F. C. Delori, and A. P. Adamis, "Diffusion of High Molecular Weight Compounds through Sclera".
37. Rehmann, M. S., K. M. Skeens, P. M. Kharkar, E. M. Ford, E. Maverakis, K. H. Lee, and A. M. Kloxin, "Tuning and Predicting Mesh Size and Protein Release from Step Growth Hydrogels", *Biomacromolecules*, Vol. 18, No. 10, pp. 3131–3142, 2017.

APPENDIX A: ADDITIONAL DATA

150kD FITC-Labeled dextran release from 10k-HG hydrogel in 1 hour, amplitude sweep test showing time dependent increase in storage modulus of 10k-HG, and ^{13}C-NMR of tetra arm PEG-PDS polymers are presented in this section.

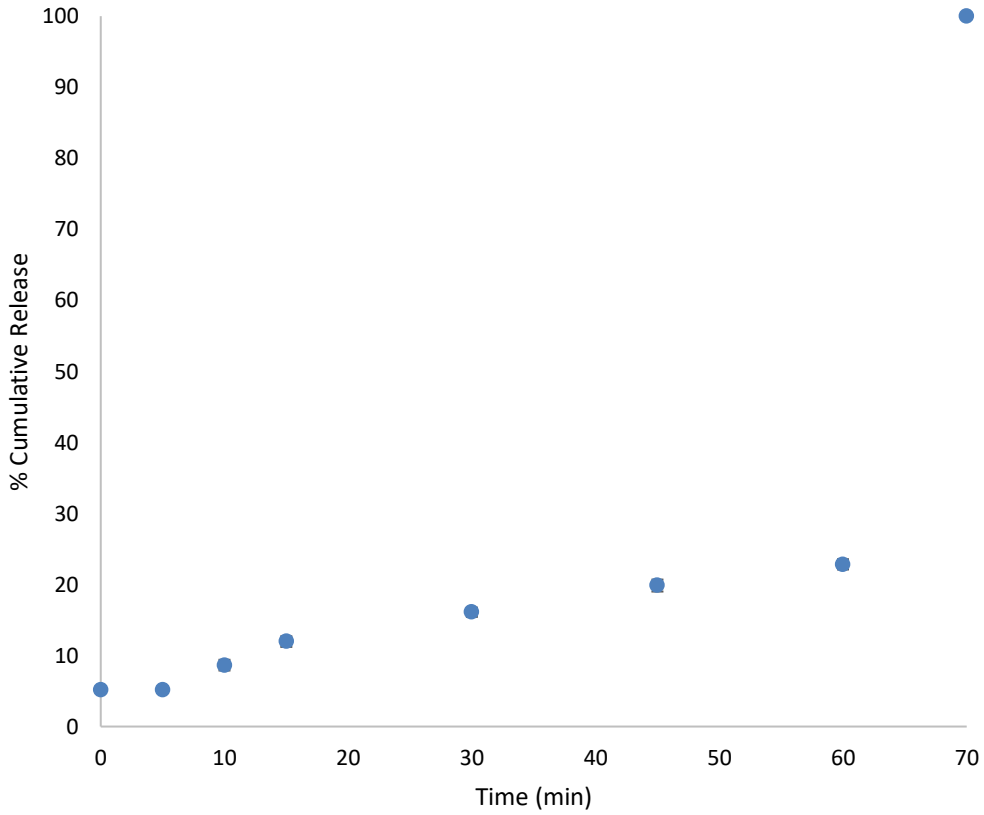

Figure A.1. 150kD FITC-Labeled dextran release from 10k-HG hydrogel in PBS (7.4) for 1 h. Release in 100mM DTT at 70th min.

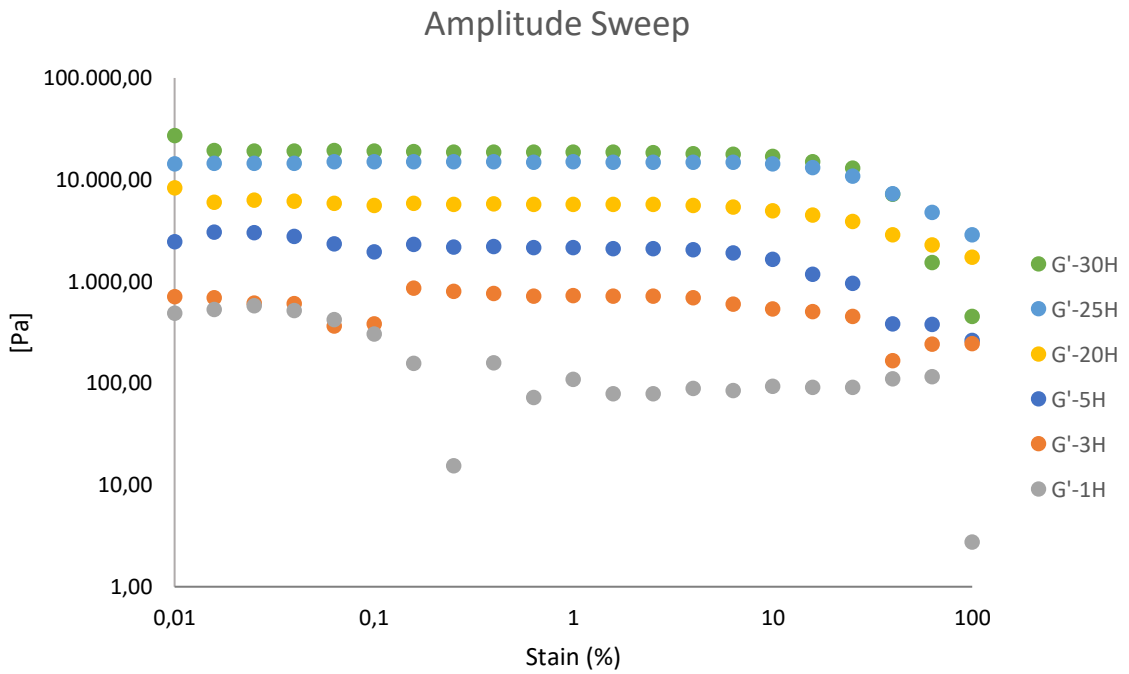

Figure A.2. Amplitude sweep test showing time dependent increase in storage modulus of 10k-HG.

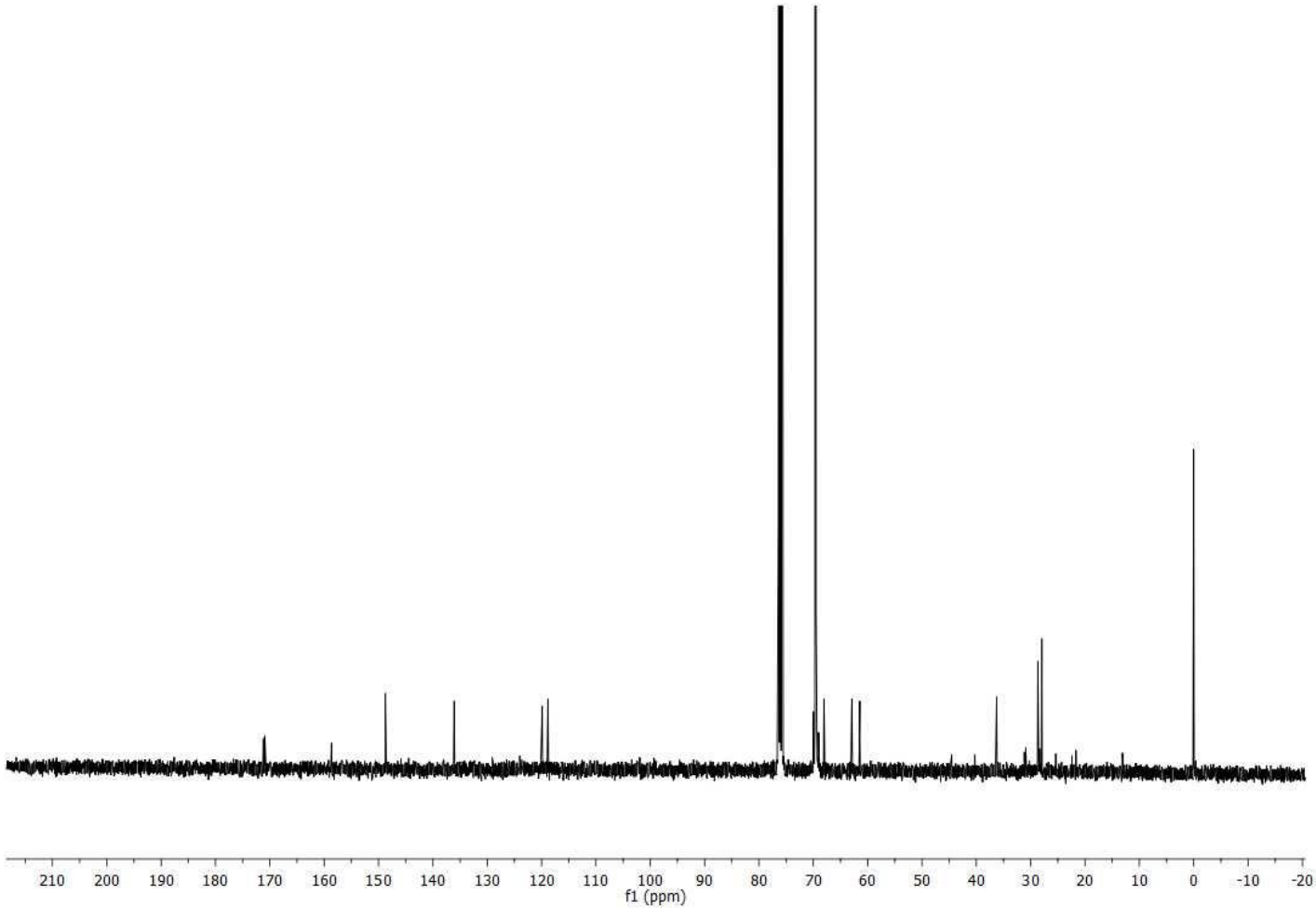

Figure A.3. ^{13}C NMR of 4 arm 10k-PEG-PDS.

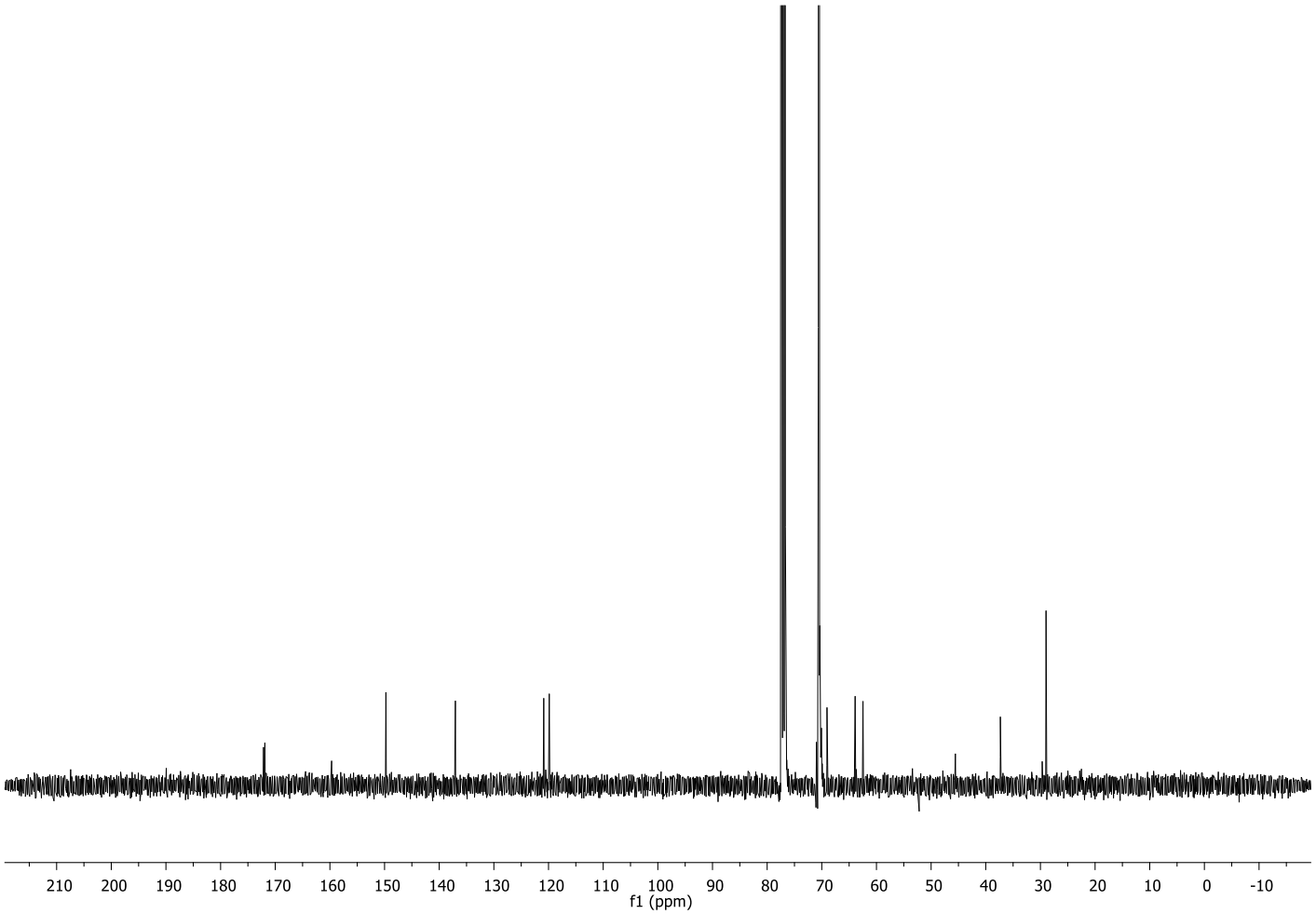

Figure A.4. ^{13}C NMR of 4 arm 20k-PEG-PDS.